Brazilian Journal of Medical and Biological Research (1998) 31: 977-1018
ISSN 0100-879X

Radioautographology: the proposal of a new concept

T. Nagata

Department of Anatomy and Cell Biology, Shinshu University School of Medicine, Matsumoto, Japan

Abstract

A new concept termed "radioautographology" is advocated. This term was synthesized from "radioautography" and "ology", expressing a new science derived from radioautography. The concept of radioautographology (RAGology) is that of a science whose objective is to localize radioactive substances in the biological structure of objects and to analyze and study the significance of these substances in the biological structure. On the other hand, the old term radioautography (RAG) is the technique used to demonstrate the pattern of localization of various radiolabeled compounds in specimens. The specimens used in biology and medicine are cells and tissues. They are fixed, sectioned and placed in contact with the radioautographic emulsions, which are exposed and developed to produce metallic silver grains. Such specimens are designated as radioautographs and the patterns of pictures made of silver grains are named radioautograms. The technicians who produce radioautographs are named radioautographers, while those who study RAGology are scientists and should be called radioautographologists. The science of RAGology can be divided into two parts, general RAGology and special RAGology, as most natural sciences usually can. General RAGology is the technology of RAG which consists of three fields of science, i.e., physics concerning radioactivity, histochemistry for the treatment of cells and tissues, and photochemistry dealing with the photographic emulsions. Special RAGology, on the other hand, consists of applications of general RAGology. The applications can be classified into several scientific fields, i.e., cellular and molecular biology, anatomy, histology, embryology, pathology and pharmacology. Studies carried out in our laboratory are summarized and reviewed. All the results obtained from such applications should be systematized as a new field of science in the future.

Correspondence
T. Nagata
Department of Anatomy and Cell Biology
Shinshu University
School of Medicine
Matsumoto 390
Japan
Fax: +81-263-33-6458

Research supported in part by Grants-in-Aid for Scientific Research from the Ministry of Education, Science and Culture of Japan, JEOL Co. Ltd. and FAPESP.

Presented at the 5th International Symposium on Radioautography, São Paulo, SP, Brasil, August 24-26, 1997.

Received July 11, 1997
Accepted May 21, 1998

Key words
- Light microscopy
- Electron microscopy
- Radioautography
- Technique
- Application

1. Introduction

The term radioautography (RAG) means the technique used to demonstrate the pattern of localization of various compounds labeled with radioactive isotopes in specimens (1). The specimens used in biology and medicine are usually cells and tissues which contain radioactive substances. They are fixed, sectioned and placed in contact with the radioautographic emulsions, which are exposed and developed to produce metallic silver grains. Such specimens are designated as radioautographs and the patterns of pictures made of silver grains are named radioautograms. Other terms such as autora-

diography, autoradiographs and autoradiograms are sometimes used alternatively (2).

Historically, the principle of radioautography was first reported by Becquerel (1896) one year after the famous discovery of X-rays by Roentgen (1895) who produced the first radiogram. This was a negative picture (white images on a black background) produced on photographic plates after the penetration of X-rays through the tissues. Becquerel found that photographic plates were activated by radiations from uranium which produced positive images (black images on a white background) after development of the plates. He first gave a talk at the annual meeting of the Paris Academy in 1896. This picture was regarded as the first radioautogram produced by radiation from the minerals. Later, London (3) reported that he could produce the picture of a frog which incorporated radium and which was placed on a photographic plate. This report appears to be the first radioautograph obtained from animal tissues. However, London (3) did not use any term for this picture. The first radioautograph from the human body was obtained by Kotzareff (4) who, when treating a patient suffering from metastatic cancer of the iliac bone with radium, placed a photographic plate on the bone and obtained a picture of the bone after photographic development. He named the picture radiumgraphie or curiegraphie after Curie. This nomenclature, however, was not used by other scientists. Lacassagne and Lattés (5) reported that the radiation emitted by radium or polonium given to rabbits could be detected on photographic plates applied to the sectioned smooth surface of paraffin blocks of embedded rabbit organs. These pictures surprised the scientist by demonstrating the distribution of radioactive substances in the organs but they did not provide good resolution. It was Lacassagne who first named these pictures autohisto-radiographie. This term was later abbreviated to autoradiography. One of his students, Leblond (6,7), moved to North America (USA and Canada) and developed a new technique to paint the tissue sections which contained radioactive compounds with warmed liquid photographic emulsion using a camel's hair brush, thus obtaining a better resolution. Pelc (8) used the stripping film method, while Joftes and Warren (9) developed the dipping method and used the term autoradiography originating from the word autohisto-radioautography used by Lacassagne. Leblond first used the term radioactive autography according to Lacassagne in the 1940's, but he later proposed to use the term radioautography by condensing the words radioactive autography into radioautography which has been used since the 1950's (10). The above historical facts tell us how the two kinds of terms were developed.

As was described above from the historical viewpoint, the two terms, radioautography and autoradiography, are originally due to the two words radioactive autography or autohisto-radiography. The two terms are now generally regarded as synonyms. However, the author prefers the term radioautography because of etymological reasons (2). In order to select terminology in scientific description, the preference for a term should depend on the etymological meaning of this term. The etymological difference between the two terms, radioautography and autoradiography, is as follows.

Radioautography is the autograph produced by radiation. It is a technique used to demonstrate the patterns of localization of radioactive substances in various specimens. The specimen which consists of tissues and cells in contact with the photographic emulsion containing developed silver grains is called "radioautograph", while the pattern of silver grains on the radioautograph is called "radioautogram" and the procedure used to produce radioautographs is designated as "radioautography". A radioautograph is an autograph produced by radiation. An autograph is a positive picture. There-

fore, etymologically the term radioautogram means the positive picture produced by radiation which is emitted from the object itself resulting in the autogram. In contrast, in the word autoradiogram the suffix auto means automatic, while the term radiogram means the picture of the object which is penetrated by rays resulting in negative images such as chest X-ray films. Thus, autoradiogram etymologically means a negative picture of the specimen produced automatically with radiation emitted from another radiation source away from the specimens. Anyhow, it is now accepted that the terms radioautography and autoradiography are synonyms (2).

On the other hand, the term radioautography or autoradiography means only the technique used to demonstrate the patterns of silver grains in specimens. Radioautography is only the technique used to produce the specimens (radioautographs) in order to demonstrate the pictures (radioautograms). In contrast, the present author now proposes a new concept, named "radioautographology". This new term was coined from "radioautography" and "ology", expressing a new science derived from radioautography. The concept of radioautographology (RAGology) is that of a science whose objective is the localization of radioactive substances in the structure of the objects and to analyze and study the significance of these substances in the structure (11).

RAGology can be divided into two parts, general RAGology and special RAGology, as most natural sciences usually can. General RAGology is the technology of RAG which consists of three fields of sciences, i.e., physics concerning radioactivity, histochemistry for the treatment of cells and tissues, and photochemistry dealing with the photographic emulsions.

Since experimentally produced radioautograms include a variety of specimens, i.e., human biopsy material, experimental animal tissues and cells or even whole bodies of small animals, the size of the specimens varies according to the samples. Larger specimens such as whole bodies or large organs are designated as macro-radioautograms which are observed with the unaided eye. In contrast, small samples such as small pieces of tissues or cells are observed under the light or electron microscope and are called microscopic radioautography. Macroscopic radioautography can be classified into two levels, whole body radioautography and organ radioautography, while the microscopic radioautography can be classified into light microscopic radioautography (LMRAG) and electron microscopic radioautography (EMRAG). These two types of radioautography are divided into two categories, soluble compound radioautography and insoluble compound radioautography, on the basis of the solubility of the radioactive compounds (4). The classifications of these two combinations are listed in Table 1. Thus, all radioautographs can be classified into 8 categories. These technologies should be designated as general RAGology.

Special RAGology, on the other hand, consists of applications of general RAGology to biology and medicine (12). From the viewpoint of radioactive compounds, it can be classified into insoluble and soluble RAG. The former concerns macromolecules such as DNA, RNA, proteins, sugars or lipids, while the latter concerns small molecules such as hormones, neurotransmitters, vitamins, inorganic substances, drugs and toxins. The applications of RAG to biology and medicine can also be classified into several

Table 1 - Classification of radioautography.

	Macroradioautography		Microradioautography	
	whole body	organ	LM	EM
Insoluble RAG	insoluble whole body RAG	insoluble organ RAG	insoluble LMRAG	insoluble EMRAG
Soluble RAG	soluble whole body RAG	soluble organ RAG	soluble LMRAG	soluble EMRAG

scientific fields, i.e., cellular and molecular biology, anatomy, histology, embryology, pathology and pharmacology. All the results obtained from such applications should be systematized as a new field of science designated as special RAGology.

The present paper is a review of general RAGology including the techniques of light and electron microscopic radioautography which were developed in our laboratory as well as special RAGology including the results applied to histology, histopathology and pharmacology of organ systems in animals and humans in our laboratory over the past 40 years.

2. General radioautographology

The science named radioautographology deals with the technology of radioautography and the applications of these techniques to various objects. It demonstrates the sites of incorporation, syntheses and discharge of various substances in living organisms by macroscopic and microscopic radioautography to localize intracellular sites of metabolism at the cellular and organelle levels in various objects. This technology should be designated as general radioautographology and includes all the natural sciences involved in the preparation of the specimens which contain radioactive compounds, the procedures for tissue preparations and the methods used to place tissues in contact with the photographic emulsions, followed by exposure for a certain period of time to produce the latent images of the radioactive substances in the specimens. The emulsion is then developed to produce the silver metal grains, thus permitting a comparison of the specimens and radioautograms in order to determine the localization of radioactive substances in the specimens. In order to carry out these procedures, three fields of knowledge, i.e., physics concerning radioactivity, histology and histochemistry dealing with the fixation, embedding, sectioning and staining of tissues and cells, and photographic chemistry treating photographic emulsions are necessary.

Table 2 - Radioisotopes used in microscopic radioautography.

Nuclide	Half-life	Rays emitted	Particle energy (KeV)
^{3}H	12.5 years	beta	18.5
^{14}C	5760 years	beta	155
^{32}P	14.2 days	beta	1710
^{35}S	87 days	beta	167
^{45}Ca	165 days	beta	250
^{56}Fe	3 years	Auger electron	14
^{125}I	60 days	Auger electron	35
^{203}Hg	45 days	beta	208

2.1. Physics of radioactive substances

2.1.1. Radioactive isotopes

The radioactive compounds used in radioautography are mainly composed of inorganic or organic compounds which are artificially labeled with radioisotopes (RI) and can be incorporated into human or animal bodies. The radioactivity emitted from the radioactive isotopes is divided into three kinds of rays, i.e., alpha, beta and gamma rays. The alpha ray is the helium nucleus in nature and has low energy, weak penetrability, strongest ionization and the shortest range (several μm). The beta ray is the electron and has medium energy, medium penetrability, medium ionization and a shorter range (μm-mm), while the gamma ray is the electromagnetic wave and has high energy, strong penetrability, low ionization and the longest range (m). Among these 3 rays, the beta ray is the best for radioautography because of its shorter range and strong ionization. The various kinds of RI used for radioautography are listed in Table 1. Among them, ^{3}H, ^{14}C, ^{35}S and ^{125}I are very often utilized for both macro- and microradioautography because they can be used to label various inorganic compounds

habitually used in biological and medical research. Since the radioactivity of the respective RI decreases time-dependently but never reaches zero, the life of an RI is defined as half-life which is the time required for the RI to lose 50% of its initial radioactivity. The half lives of ^{3}H or ^{14}C are longer (years) than those of ^{35}S or ^{125}I (days) as listed in Table 2, so that the experiments using shorter half-life compounds should be completed within a shorter period.

2.1.2. RI-labeled compounds

In histology, histopathology and pharmacology the RI-labeled compounds used for radioautography can be classified into 2 categories, i.e., the precursors which are incorporated into macromolecules such as nucleic acids (DNA and RNA), proteins, glucides and lipids, and the other target tracers which are small molecular compounds such as hormones, neurotransmitters, vitamins, inorganic substances, drugs and others (Table 3). All RI should be treated only in the RI laboratories according to the regulations concerning radiation damage enforced in each country.

2.1.3. Administration of radioactive compounds

In order to study the localization of radioactive compounds in animal bodies, compounds labeled with a specific RI are usually administered orally to small animals such as rats and mice or by injection given subcutaneously, intramuscularly, intravenously or intraperitoneally. For the purpose of demonstrating macromolecular synthesis, animals were injected intraperitoneally with radioactive precursors for macromolecular synthesis at concentrations ranging from 1 to 50 µCi (37-1850 kBq)/gram body weight for macro- and for LMRAG or 10-100 µCi (370-3700 kBq)/g body weight depending on the characteristics of the compounds and RI used. The RI-labeled precursors used in our experiments were [^{3}H]-4-thymidine (Amersham, Buckinghamshire, England; specific activity 877 GBq/mM) for DNA synthesis, [^{3}H]-uridine (Amersham; 1.11 TBq/mM) for RNA, [^{3}H]-4,5-leucine (Amersham; 1.04 TBq/mM) and [^{3}H]-taurine (New England Nuclear, Boston, MA, USA; specific activity 74 GBq/mM) for proteins, [^{3}H]-1-glucosamine (Amersham; 105 GBq/mM) for polysaccharides, [^{35}S]-sulfuric acid (Amersham; 1.11 TBq/mM) for mucosubstances, and [^{3}H]-1,2,3-glycerol (Amersham; 7.4 GBq/mM) for lipids.

Sometimes *in vitro* labeling can be carried out in cultured cells, both established cell lines or primary culture and tissue blocks obtained from human biopsy or necropsy material, in media containing radioactive compounds at concentrations of 1-100 µCi (37-3700 kBq)/ml medium, using a CO_2 incubator at 37°C with 5% CO_2 in air under normal or pathological conditions, for time intervals ranging from several minutes up to several hours.

Table 3 - Radio-labeled compounds used in microscopic radioautography.

Macromolecular precursor	Radio-labeled compounds
Nucleic acids	
DNA	[^{3}H]-thymidine
RNA	[^{3}H]-uridine
Proteins	
secretory granules	[^{3}H]-glycine, [^{3}H]-leucine, etc.
collagen	[^{3}H]-proline, [^{3}H]-hydroxyproline
Glucides	
simple polysaccharides	[^{3}H]-glucose, [^{3}H]-glucosamine, etc.
mucosubstances	$^{35}SO_4$
Lipids	[^{3}H]-glycerol, [^{3}H]-fatty acids, etc.
Target tracers (low molecular weight compounds)	
Hormones	[^{3}H]-steroids, [^{3}H]-insulin, etc.
Neurotransmitters	[^{3}H]-GABA, [^{3}H]-dopamine, etc.
Vitamins	[^{3}H]-vitamin A, B, C, D, etc.
Inorganic substances	$^{22}NaCl$, $^{45}CaCl_2$, $^{203}HgCl_2$, etc.
Drugs	[^{3}H]-antibiotics, [^{3}H]-anti-allergics, etc.
Toxins and others	[^{3}H]-ouabain, [^{3}H]-strychnine, etc.

2.2. Histology and histochemistry for radioautography

2.2.1. Animal treatment and tissue processing

Small animals such as mice and rats are anesthetized by intraperitoneal injections with pentobarbital sodium (Nembutal, Abbott Laboratories, Chicago, IL, USA), after the administration of radioactive compounds by either oral administration or injection, and are sacrificed at a given time, usually 1 h after RI administration, either by decapitation or by perfusion via the left ventricles of the heart with 2.5% glutaraldehyde in 0.1 M cacodylate buffer, pH 7.2, depending on whether insoluble or soluble radioautography will be carried out. For conventional insoluble radioautography perfusion fixation can be used and the tissues from various organs are dissected out, cut into small pieces (1 x 1 x 1 mm), soaked in the same glutaraldehyde fixative at 4°C for 1 h and postfixed in 1% osmium tetroxide in the same buffer for 1 h, dehydrated with graded ethanol and embedded in epoxy resin (Epon 812 or Epok 812, Oken Co., Tokyo, Japan). In contrast, *in vitro* labeling of cultured cells and tissue blocks obtained from either animal or human biopsy material are incubated in media containing radioactive compounds, using a CO_2 incubator under normal conditions at 37°C for a given time, usually 1 h or up to a few hours. They are then rinsed in Hanks' solution, fixed in the same buffered glutaraldehyde and osmium tetroxide solutions, dehydrated and embedded in epoxy resin as described above.

For soluble radioautography, however, perfusion fixation cannot be used. The whole bodies of the small animals or organs and tissues obtained after decapitation without using any perfusion methods should be immediately cryo-fixed by the metal contact method or by the method of immersion in liquid nitrogen and processed by cryo-sectioning or freeze-drying or freeze-substitution (13). Macroscopic RAG of whole bodies of small animals usually employs cryofixation by immersion in a dry ice and acetone mixture and cryo-sectioning with a large cryostat microtome (14).

Tissues embedded in epoxy resin can be used for either LMRAG or EMRAG. For LMRAG, 2-µm thick sections are cut with an ultramicrotome, picked up onto clean glass slides and warmed for extension and drying. For electron microscopy, ultrathin sections of 100-nm thickness are cut and usually examined under a conventional transmission electron microscope with the accelerating voltage at 100 kV. It is generally accepted that the thinner the section the better the resolution, but the less the radioactivity it contains and the longer the exposure time for radioautography. If an intermediate high voltage electron microscope is available with accelerating voltages of 200, 300 or 400 kV, thicker sections of 200 or 300 nm can be used. We prefer to use semithin 200-nm thick sections at 400 kV in order to shorten the exposure time (15). Semithin sections are cut with a Porter-Blum MT-2B ultramicrotome (Dupont-Sorvall, Newtown, CN, USA). Ultramicrotomes of the mechanical feeding type are preferable to the thermal feeding type because of the accuracy of the section thickness, which affects the number of silver grains by radioautography. Ultrathin or semithin sections are picked up onto either platinum or gold grid meshes in order to prevent the copper meshes from rusting through the histologic and radioautographic treatment especially during development. Alternatively, collodion-coated copper grid meshes can be used. For collodion coating, copper grid meshes (100-200 meshes) are soaked in 2% collodion solution for a few minutes, spread on filter paper in a Petri dish and dried at 37°C for a few hours in an incubator.

2.2.2. Fixation of tissues and cells

We have developed simple routine techniques to demonstrate insoluble compounds in various cells and tissues of experimental animals and to quantify the contents of newly synthesized macromolecules in each cell and cell organelle by both light and electron microscopy. The localization of silver grains developed by means of ordinary radioautography, however, demonstrates only the insoluble radioactive substances bound to the macromolecules fixed in the cell with the chemical fixatives used (1). In contrast, radioisotopes bound to the small molecules which are not fixed with ordinary chemical fixatives are washed away by conventional routine procedures such as fixation, dehydration, embedding, sectioning, and radioautographic procedures, so that these compounds cannot be demonstrated. Ordinary radioautographic procedures can be designated as wet-mounting radioautography, since the tissues are processed by both conventional wet treatments and by applying wet radioautographic emulsions to the specimens. In order to demonstrate any soluble radioactive compound, special techniques are required in accordance with the characteristics of the radioisotopes used for radioautography (Table 4). The techniques for microscopic radioautography developed in our laboratory can be divided into 2 categories, i.e., wet-mounting radioautography for insoluble compounds resulting from macromolecular synthesis and dry-mounting radioautography for soluble compounds such as small molecular compounds, and each can be subdivided into two methods, i.e., light microscopy and electron microscopy (Table 4).

2.2.2.1. Chemical fixation for wet-mounting radioautography

Small animals such as mice and rats are anesthetized and sacrificed either by decapitation or by perfusion via the left ventricle of the heart with 2.5% glutaraldehyde in 0.1 M cacodylate buffer, pH 7.2. The tissues from various organs are removed, cut into small pieces, soaked in the same glutaraldehyde fixative at 4°C for 1 h and postfixed in 1% osmium tetroxide in the same buffer for 1 h, dehydrated with graded ethanol and embedded in epoxy resin. On the other hand, cultured cells and tissue blocks, incubated in media containing radioactive compounds *in*

Table 4 - Principle techniques for microscopic radioautography demonstrating soluble and insoluble compounds.

a, Radioautography for conventional insoluble compounds. b, Precipitation procedure of radioautography for soluble compounds. c, Freezing procedure of radioautography for soluble compounds.

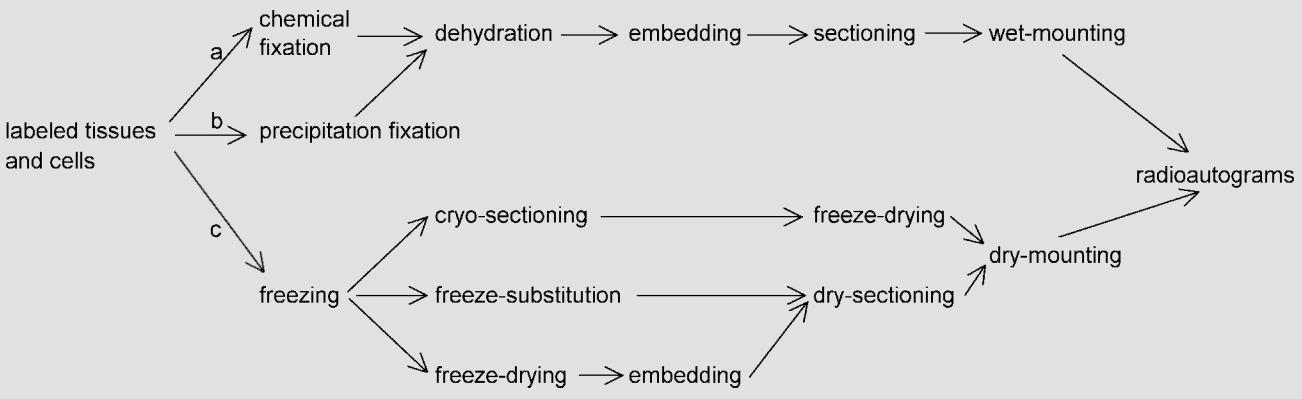

vitro, using a CO_2 incubator under normal conditions at 37°C for given times, are rinsed in Hanks' solution, fixed in the same buffered glutaraldehyde and osmium tetroxide solutions, dehydrated and embedded in epoxy resin as described above. The tissue blocks are cut with an ultratome for either LM (2 μm thick) or EM (0.1-2 μm) and picked up onto either glass slides or grid meshes using water. In some cases, the whole mount cells on glass coverslips or coated meshes are fixed, dried and used for wet-mounting radioautography to observe the whole cells without sectioning (15). In order to observe isolated cells obtained from the tissues *in vivo*, small tissue blocks are oscillated in Ranvier's alcohol and isolated, smeared on glass slides, fixed in Carnoy's fluid, and wet-mounted for LMRAG (16).

2.2.2.2. Chemical fixation for soluble compounds

The techniques of radioautography of soluble compounds can be theoretically classified into two categories according to the fixation used, as shown in Table 4 (17,18). In the precipitation method, the labeled soluble compound is fixed in a mixture containing a substance which reacts with the soluble radioactive compounds forming a precipitate, so that the fixed tissues can be processed by routine histological procedures followed by a routine wet-mounting radioautography to demonstrate the labeled precipitation. This principle was first used to detect soluble ^{45}Ca by Nagata and Shimamura (19-21) in light microscopic radioautography of several tissues fixed in formaldehyde solution containing ammonium oxalate to form a calcium oxalate precipitate. At the electron microscopic level, Mizuhira et al. (22) later used this method by fixing the tissues labeled with [^{3}H]-thiamine with a glutaraldehyde solution containing platinum chloride to form thiamine-$PtCl_6$ precipitation, or fixing labeled [^{3}H]-cholesterol with a mixture containing digitonin. This procedure, however, is limited to the radioactive compounds which can be precipitated with any other specific compounds. Moreover, there are many possibilities of diffusion of the labeled compounds when they are precipitated with the fixatives.

2.2.2.3. Cryo-fixation for soluble compounds

By the freezing method, on the other hand, the labeled tissues are quickly frozen in a liquid such as isopentane or propane cooled to its melting point with liquid nitrogen. The tissues can then be cut by cryomicrotomy. At the light microscopy level, the frozen tissues can be cut with a cryostat and the frozen sections are placed in contact with radioautographic emulsions by various methods. At the light microscopy level, the frozen tissues can be cut with a cryostat at a thickness around 20-30 μm and the frozen sections are placed in contact with radioautographic emulsions by various techniques. Many papers have been published on this problem. We first used a large-wire loop to produce dry films which were air-dried and applied to cryostat sections placed on glass slides (23). This procedure is very convenient and will be described in detail. At the electron microscopy level, however, only a few papers have been published on the principle of cryo-ultramicrotomy. Appleton (24) and Christensen (25) discussed the possibilities of this method but they did not demonstrate the results, while we (17) reported the results for the first time. In contrast, Mizuhira et al. (26), and Futaesaku and Mizuhira (27) reported a new technique for ultramicrotomy utilizing interposed films, which, however, is not an ideal procedure because it employs cryosectioning after the tissues are immersed in sucrose solution. The cryosections are then picked up with sucrose droplets and placed in contact with wet radioautographic emulsion.

On the other hand, freeze-dried or freeze-

substituted tissues can be embedded in paraffin or resin for light microscopy and dry sections can be mounted on precoated slides. Edwards and Udupa (28) and Smitherman et al. (29) used freeze-dried and paraffin-embedded sections. Miller Jr. et al. (30) applied the wire loop method as part of the dry-mounting procedure at the light microscopy level. We improved this technique first at the light microscopy level (23) and then applied it at the electron microscopy level (17). Stirling and Kinter (31) embedded freeze-dried tissues in silicon-araldite and the plastic sections were wet-mounted with a dropping procedure but not by dry-mounting.

To demonstrate soluble low molecular weight compounds, cryo-fixation and dry-mounting radioautography should be routinely employed for both LMRAG and EMRAG.

2.2.2.3.1. Preparation of tissue blocks

After the tissues are removed without using any solution from the experimental animals previously injected with radioactive compounds, they are trimmed to a size as small as 1 x 0.5 x 0.5 mm with two pieces of razor blades on a plate cooled to 0°C with ice and water. The tissue blocks are attached to small pieces of aluminum foil, 5 x 5 mm in size (13), or directly to the surface of a metal block. Cultured cells are centrifuged at 500 rpm for 10 min after incubation with media containing radioactive compounds, and the pellet is placed on a piece of aluminum foil or on metal blocks.

2.2.2.3.2. Freezing procedure

For quick fixing by cryo-fixation, we soak the tissues in a quenching fluid which is cooled with a cooling agent. The quenching fluids we usually employ are propane (melting point, -169°C), isopentane (-161°C), or hexane (-94°C). These reagents are liquids at low temperatures and conduct heat very well. They also bubble when they contact tissues. Among them, propane is explosive, while hexane has a rather higher melting point. Therefore, isopentane is very often used (13). Instead of quenching fluids, a pure copper block is sometimes used in direct contact with the tissues.

The following substances or mixtures of two substances are generally used as cooling agents: liquid helium (boiling point, -269°C), liquid nitrogen (-196°C), liquid air (-190°C), dry ice and ether (-60°C), and dry ice and nonane (-53°C). Among these, liquid nitrogen is most frequently used. We usually employ the combination of isopentane or propane as the quenching fluid and liquid nitrogen as the cooling agent, or a copper block as metal contact and liquid nitrogen as the cooling agent. Cryo-instruments such as RF-2 (Eiko, Tokyo, Japan), JFD-RFA (JEOL, Tokyo, Japan), cryoblock or cryovacublock (Reichert-Jung, Jena, Germany) have recently become commercially available. Liquid nitrogen (200-300 ml) is carefully poured into a Dewer flask. A 50-ml beaker is placed in liquid nitrogen, and 20-30 ml of isopentane or propane is poured into the beaker. We prefer isopentane to propane. Within a few minutes the liquid isopentane begins to solidify at its melting point of -161°C as it is cooled by the liquid nitrogen at -196°C. The tissue blocks or free cells adhering to a small piece of aluminum foil are plunged quickly in the isopentane with a pair of forceps. The frozen tissues are then removed from the isopentane using a small cup made with a piece of aluminum foil 3 cm x 3 cm in size, molded with a No. 00 gelatin capsule in order to prevent ice crystal formation, transferred to liquid nitrogen in a Dewer flask, and stored in liquid nitrogen until processing. In this process, if the tissues are exposed to air, ice crystals will grow larger, and the fine structure will be damaged. The frozen tissues are then processed by freeze-drying or freeze-substitution procedures. When the metal contact method is employed, using

cryo-instruments, frozen tissues are removed from the copper blocks and also stored in liquid nitrogen.

2.2.2.3.3. Cryo-sectioning

The frozen tissues can be cut directly by cryo-sectioning without any embedding. The procedures for cryo-sectioning can be divided into light microscopy and electron microscopy.

2.2.2.3.3.1. Light microscopic cryo-sectioning

The frozen tissues can be cut with a cryostat at -80°C, and the frozen sections are then placed on glass slides in contact with radioautographic emulsions for light microscopy. Various techniques are employed. Kinter et al. (32) placed sections directly on the photographic plates and clamped them for exposure. Fitzgerald (33) applied dry films to sections mounted on slides. Appleton (24) placed sections on precoated slides at low temperature. Stumpf and Roth (34-36) transferred freeze-dried sections on either siliconized slides or Teflon slides. Hammarstrom et al. (37) used cellophane tapes to attach sections to plates. Since Appleton (24) first applied cryostat sections to precoated slides at very low temperature, many investigators such as Rogers et al. (38) have used this technique at the light microscope level. All of these techniques require handling of the sections, glass slides and emulsions in the dark room. When cryostat sections picked up onto precoated slides are air-dried at room temperature, the sections melt and cause diffusion of soluble compounds. This procedure is called thaw-mount radioautography and is applicable when the diffusion is negligible.

In contrast, we use the cryostat in a conventional bright room and then coat the cryosections with the emulsion in a darkroom using the large wire loop method (23). We use a conventional rotary type cryostat. The frozen tissues are transferred to a cryostat kept at around -30°C and dry sections of 20-30 μm are cut. They are transferred to glass slides and either air-dried at room temperature or freeze-dried at -30°C for a few hours. The procedure for coating the slides with dry emulsion film by the large wire loop method will be described later.

2.2.2.3.3.2. Electron microscopic cryo-sectioning

The technique of ultrathin cryo-sectioning, or simply cryo-ultramicrotomy, was first reported by Bernhard and Leduc (39) and was later improved by Tokuyasu (40) employing preincubation in sucrose solution and picking up sections with sucrose droplets. For radioautography, however, his technique is not applicable because of the diffusion of radiolabeled compounds. We use an LKB ultratome 4800 equipped with an LKB cryokit 14800 or an LKB-NOVA (LKB, Bromma, Sweden). Other types of ultramicrotomes such as DuPont-Sorvall or Reichert-Jung with cryokits can also be used. The temperature of the specimens is usually set at -100°C to -120°C and that of the glass knives at -80°C to -100°C. The optimal temperature depends on the kind of tissue used. Dry sections are picked up with dry eyelash probes onto grids, covered with another grid as a sandwich and pressed with copper rods according to Christensen (25) or Sakai et al. (41). The authors use a modified apparatus of the Sakai type. Grids used for this purpose are coated with collodion applied by soaking in 1% collodion solution and dried at 37°C for 1 h. As controls, wet sections are picked up with sucrose droplets (42). Grids carrying dry sections are dried by freeze-drying at -50°C for 24 h, as done in the freeze-drying procedure of tissue blocks described above. Among the drying procedures tested, i.e., freeze-drying, freeze-substitution, and air-drying, the freeze-drying procedure was the best from the viewpoint of preservation of

both cell structure and radioisotopes (13). In order to freeze-dry cryosections, we use a rotary cryotransfer apparatus. The rotary disc, which has spaces for 5 grids with cryosections, is changed every 5 grid and transferred to a carrier, which consists of a tube and a cylinder containing up to 5 discs on its shelves, for a total of 25 grids (13). The carrier is transferred to the desiccator of the freeze-drying apparatus, which is operated for 3 h at -80°C. After drying the cryosections are coated with carbon and processed by the dry-mounting radioautographic procedure. Cryotransfer apparatuses have recently become commercially available as attachments of cryo-kit-equipped ultramicrotomes such as LKB, Sorvall or Reichert instruments.

2.2.2.3.4. Freeze-drying procedure

The freeze-drying technique was first used by Altmann (43), and was then applied to light and electron microscopy by Gersh (44,45). The freeze-drying apparatus we use was designed and constructed in our laboratory (13,16). It consists of a cold trap, a desiccator, which is set in the cold trap, three Geisler discharge and ionization vacuum gauges, and two rotary and oil diffusion vacuum pumps. The cold trap consists of a stainless steel cylinder containing liquid nitrogen. The desiccator, which is set in the cold trap, has 96 sets of thermoelements which can be controlled with electric current at temperatures between -80 and +60°C. The whole apparatus is capable of maintaining a pressure of less than 10^{-6} Torr. A similar apparatus is now commercially available from several manufacturers. The frozen tissues are transferred to the freeze-drying apparatus in a small aluminum cup. The freeze-drying should be carried out at first with the operation of the rotary pump for about an hour until the pressure reaches 10^{-3} Torr. The two pumps (RP and DP) are then operated for about 24 h to complete drying, while the desiccator is kept at -80°C. After the completion of freeze-drying, the temperature is slowly increased over several hours by adjusting the electric current of thermoelement, so that the whole drying procedure takes about 30 h for tissue blocks. When cryo-sections on grids are used, however, freeze-drying for only 12 h is sufficient. Before completion of the procedure, the epoxy embedding mixture is placed in the dripping unit which should be evacuated for 10 min by means of another rotary pump at a pressure of 10^{-3} Torr. After completion of drying, the embedding medium, epoxy resin mixture, is dripped down into the specimen chamber, the tissues are infiltrated and the two pumps are stopped. When the drying procedure is completed, the tissues adhering to the aluminum foil will sink in the embedding medium. Fixation is not required before embedding, although Pearse (46) maintains that the unfixed freeze-dried tissues are easily damaged. When fixation is preferable before embedding in order to enhance contrast, freeze-dried tissues can be exposed to osmium vapor for 30 min in a tight jar containing a small piece of osmium tetroxide crystal. Freeze-dried tissues are taken out and infiltrated with fresh embedding medium overnight at room temperature, and polymerized at 35°C, 45°C and 60°C for 12 h each by the method of Luft (47). When cultured cells or cryo-sections on grids are freeze-dried, no embedding is necessary. The cultured cells freeze-dried on grids are processed directly by radioautography and can be observed by high voltage electron microscopy (15,48,49).

2.2.2.3.5. Freeze-substitution

The technique of freeze-substitution or freeze-thawing was first applied to light microscopy by Simpson (50) and was later developed by Lison (51). At the electron microscopy level, several papers describing the morphology of freeze-substituted cells

have been published (52,53). The principle of freeze-substitution is to dehydrate the frozen tissues in a solvent at very low temperature without thawing the tissues, and to substitute the ice with the solvent. The usual solvents are acetone, ethanol or ether. The coolants used are a dry ice-acetone mixture (-78°C) or dry ice-ethanol (-78°C). We applied this principle to radioautography for the first time (54). The routine procedure is as follows.

1) Dry ice and acetone are mixed in a Dewer flask. 2) A small test tube or sample tube containing 20-30 ml of absolute acetone is placed in the Dewer flask and cooled to -78°C. 3) Tissues are frozen according to the procedure described above in liquid nitrogen, and transferred with aluminum foil cups to the test tube containing absolute acetone. 4) The transferred tissues are kept in the substituting fluid for 72 h to exchange the ice with the solvent. The present authors use a deep freezer (Tabai, Tokyo, Japan) in which the Dewer flask is stored and the temperature is kept at -80°C. 5) After the substitution of ice with solvent is completed, the temperature is gradually raised to 20°C over several hours. The tissues are transferred to an Epon/acetone mixture, then processed through Epon mixtures and polymerized. In general, it is useful to use cryoprotective agents such as glycerin, DMSO, or sucrose in order to reduce ice crystal formation artifacts. However, for the purpose of demonstrating soluble radioactive compounds by means of radioautography, it is preferable not to employ such techniques. Recently, freeze-substitution instruments such as CS-auto (Reichert-Jung) which can be controlled automatically have become commercially available.

2.2.2.3.6. Dry sectioning of freeze-dried or freeze-substituted materials

After freeze-drying or freeze-substitution the embedded tissues should be cut dry without using any water. We usually cut dry sections from epoxy resin-embedded tissues for both light and electron microscopy without water. To section the Epon or Epok blocks of freeze-dried or freeze-substituted tissues, it is necessary to cut sections without using water in the knife trough in order to prevent diffusion artifact of labeled soluble compounds. Complete dry sectioning without any liquid is very difficult in terms of expanding dry sections. It is also difficult to pick them up onto glass slides or grid meshes. Among many knife trough liquids which we tested, ethylene glycol was the best for flotation and expansion of the dry sections (17). It wets the glass knife to the very edge but does not wet the plastic sections. It does not dissolve soluble labeled compounds. Sections are not so easily expanded on ethylene glycol as on water, but can be expanded when they are warmed with a tungsten lamp for a few minutes. They are picked up onto collodion-coated glass slides or 150 mesh grids. We use glass slides or grids which are previously coated with collodion by dipping them in 1% collodion solution and drying them at 37°C for 1 h.

2.2.3. Observation of radioautograms by microscopy

After the specimens are coated with radioautographic emulsions according to the various procedures described in the following sections, the developed radioautograms are stained and observed by light or electron microscopy.

2.2.3.1. Light microscopy

Light microscopic radioautograms are observed by either conventional transmission light microscopy or dark field incident light microscopy. By the former method silver grains appear dark together with the stained sections, so that the localization of silver grains is clear but sometimes confus-

ing due to densely stained structures such as secretory granules. Epon thick sections are usually stained with toluidine blue, while paraffin sections can be stained with conventional hematoxylin and eosin or any other routine stain after the radioautographic emulsions are developed. If the sections were stained before the application of emulsion, the staining can sometimes cause chemical background fogs. On the other hand, by the latter method silver grains appear as bright specks over the dark sections like stars in the dark sky, so that we can recognize the silver grains but cannot observe the sections well. In this case, staining is not necessary. Either method has its advantages and disadvantages. It depends on the preference of each investigator.

2.2.3.2. Electron microscopy

Electron microscopy can usually be carried out using conventional transmission electron microscopes with standard voltage around 100 kV. However, we prefer to use intermediate high voltage electron microscopes with accelerating voltages at 200, 300 or 400 kV when available in order to obtain better contrast between the silver grains and the cell structures as well as to shorten the exposure time using semithin sections which contain more RI than ultrathin sections. We use either a Hitachi H-700 electron microscope at 200 kV or a JEOL JEM-4000EX electron microscope at 300 or 400 kV (15).

2.2.3.3. Image analysis of radioautographs

To analyze these radioautograms quantitatively, we can use various kinds of image analyzers now commercially available (55,56). The number of labeled nuclei per total cell population labeled with [^{3}H]-thymidine is determined to calculate the labeling index, or the number of silver grains per cell body or per unit area labeled with other macromolecular precursors is determined to calculate the relative incorporation rates. On the other hand, direct quantification of silver grains on EMRAG is possible by using energy dispersive X-ray microanalyzers equipped with intermediate high voltage electron microscopes with either STEM or TEM modes (57).

2.3. Photochemistry and radioautographic emulsions

2.3.1. The radioautographic emulsions

The photographic emulsions for normal photography generally consist of both matrices of gelatin and photosensitive silver halide crystals which are embedded in gelatin. The nuclear emulsions used for radioautography are sensitive to radiation and consist of a gelatin matrix and silver bromide crystals. The silver bromide crystals are uniform in size ranging from 70 to 400 nm in diameter depending on their brands and are produced by several photo-industry manufacturers such as Konica (Japan), Eastman-Kodak (USA), and Ilford (UK). Several kinds of emulsions are commercially available. They are classified into four types, i.e., gel form or bulk liquid emulsions for light and electron microscopy, stripping films for LMRAG, coated plates or films for macro-RAG and LMRAG, and coated films for macro-RAG. We prefer to use bulk liquid emulsions produced by Konica Co. (Tokyo, Japan), Konica NR-M2 for LMRAG and Konica NR-H2 for EMRAG, because of their fine grains and high sensitivity. Other types of emulsions such as Kodak NTB-2, 3, 5, or Ilford K-2 and L-4 can be used alternatively.

2.3.2. The application of radioautographic emulsions to specimens

Various techniques for applying radioautographic emulsions to the specimens have been published, depending on the kinds of specimens and radioactive compounds to

be examined. The procedures are described in detail according to the methodologies employed in the following sections. After the specimens are placed in contact with the emulsions, they are kept in a cold (4°C) dark room, usually in a light-tight slide box stored in a refrigerator, for exposure for several weeks and finally developed. The development is a chemical reaction that reduces the silver bromide crystals in a developer and converts them to metallic silver grains. When the emulsion is soaked in a developer, the developer reduces the silver bromide crystals which contain specks of latent images, building up more and more metallic silver around the latent image. The size of silver grains depends on the constituents of the developer as well as the time and temperature of development. The standard developers such as Kodak D-19 or Konica SD-X1 consist of some reducing reagents such as methol and hydroquinone, which are abbreviated as MQ developers. When MQ developers are used for both LM and EMRAG, large spiral silver grains as long as a few μm are grown, which can be observed by light microscopy without problems but are too large for electron microscopy. On the contrary, when a fine grain developer such as gold latensification and phenidon developer at a low temperature and shorter time is used, small dot-like silver grains less than 1 μm in diameter are produced, which are preferable for electron microscopy (1,58).

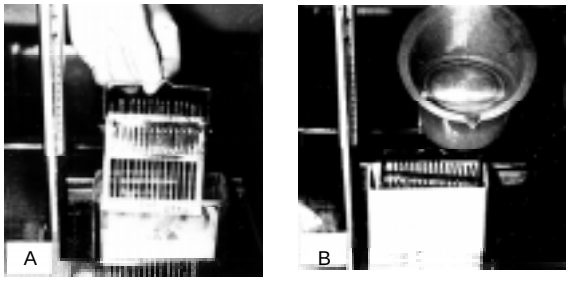

Figure 1 - The standard procedure for preparing LMRAG by wet-mounting radioautography. *A*, Bulk emulsion is melted and diluted with distilled water in a staining jar, in which a slide holder holding 15 slides is dipped and pulled up vertically. *B*, The slide holder is stored in a light-tight slide box for exposure, into which the developer is finally poured after exposure for developing all the slides at once.

2.3.2.1. Light microscopic wet-mounting radioautography

For conventional light microscopic wet-mounting radioautography, the same tissue blocks used for electron microscopy, which were fixed in buffered glutaraldehyde and osmium tetroxide solutions and then embedded in epoxy resin, are cut with a Porter-Blum MT-2B ultramicrotome at 2-μm thickness, picked up onto clean glass slides and warmed for extension and drying. Otherwise, conventional formalin fixed, paraffin-embedded tissues can be used. In order to produce many radioautograms simultaneously and also to compare them quantitatively, the following procedures, developed in our laboratory (59,60), are carried out.

1) A bottle of bulk emulsion (we use Konica NR-M2 emulsion, Konica Ltd., Tokyo, Japan), is melted in a water bath at 45°C for about 10 min, and an equal amount of distilled water is added to it and mixed for 5-10 min with a glass slide to remove all air bubbles. Then, a slide holder made of stainless steel, holding 15 glass slides which carry several thick sections, is dipped in the melted emulsion for several seconds, and then pulled up vertically for about 3 s to assure equal thickness coating (3-4 μm) over the sections (Figure 1A). The faster the speed, the thinner becomes the emulsion coating. 2) The bottom of the slide holder is wiped with a paper towel to remove excess emulsion and the slide holder is placed in an electric incubator at 28°C with a humidity of about 80%, containing a wet sponge at the bottom, and dried for 1 h. When the slides are dry, they are stored in a light-tight slide box containing a desiccant (silica gel). The edge of the box is sealed with black tape and the box is kept in a refrigerator at 4°C for exposure. 3) After an appropriate exposure time, all the slides are developed at once by pouring the developer

into the slide box (Figure 1B). We use Konica KD-X1 (formerly SD-X1) developer for Konica NR-M2 emulsion. Kodak D-19 may be used for any type of emulsion. After development, the slides are rinsed in a stop bath (2% aqueous acetic acid solution), fixed twice in a fixer (30% aqueous sodium thiosulfate solution) for 5 min, washed gently in running tap water for 10 min, and finally stained in 1% toluidine blue solution for light microscopy.

2.3.2.2. Electron microscopic wet-mounting radioautography

The same embedded tissues in epoxy resin can be used for both LMRAG and EMRAG. For EMRAG, ultrathin sections of 0.1 μm (100 nm) or semithin sections of 0.2 μm (200 nm) are cut with an ultramicrotome and picked up on collodion-coated grid meshes. The semithin sections should be observed by high voltage electron microscopy (49).

As for the radioautographic emulsions, several types of emulsions are commercially available. We use Konica NR-H2 emulsion (Konica Ltd.) because of the small sized silver bromide crystals and better sensitivity. To obtain a thin monolayer of silver bromide crystals, two techniques, dipping and wire loop methods, are now in general use. The choice lies between mounting the sections on a flat microscopic glass slide or on a grid mesh during exposure. By the former method, glass slides are covered with thin collodion films on which sections are placed and are coated with radioautographic emulsion by dipping as done in the light microscopy procedure. After exposure and photographic processing, the sections and collodion films together with the emulsion are floated off the glass slide and picked up on a grid for examining by electron microscopy. This procedure is called the flat substrate method and is highly complicated and cumbersome. On the other hand, by the latter method, sections are placed on grid meshes coated with collodion films according to the normal sectioning method and are covered with a preformed monolayer emulsion by picking up thin bubbles of molten emulsion with a wire loop and allowing them to gel before touching the grids. This is called the wire loop method. We prefer this procedure, which was developed in our laboratory, using small or larger wire loops, and appears to be rather easier. Our procedure is described in detail as follows (1,58,61).

1) A regular 1.25-cm square glass block is made from No. 4890-40 glass strips for the LKB knife maker (LKB-Produkter AB, Bromma, Sweden). A square piece of double-coated Scotch tape, 4 mm in length, is stuck on the surface of each glass block. Six grids are placed around the tape like a rosette, arranged clockwise to identify each grid (Figure 2A). The grids are vacuum coated with carbon of 10-nm thickness. 2) The radioautographic emulsion is diluted with an equal part of distilled water at 45°C. We use Konica NR-H2 emulsion from Konica (formerly Sakura) Ltd., Tokyo, Japan, but any other emulsion such as Kodak can be used. Ten ml of diluted emulsion is added to 0.2 ml of a 2% aqueous solution of dioctyl sodium sulfosuccinate (a surfactant) in order to prevent the emulsion film from bursting (14). A thin film of emulsion is obtained by dipping

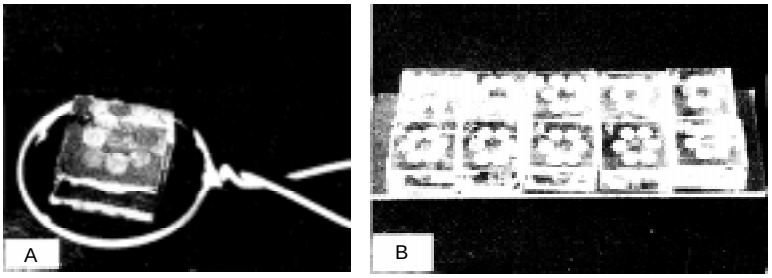

Figure 2 - The standard procedure for preparing EMRAG by wet-mounting radioautography. *A*, A large wire loop is dipped into melted emulsion and a thin film of emulsion is obtained, which is applied horizontally to a glass block on which 6 meshes, each carrying several sections, are placed. *B*, Ten glass blocks carrying 6 meshes each are attached to a glass slide with Scotch tape. Thus, several glass slides, each carrying 10 glass blocks, are stored in a slide box for exposure and finally all the meshes on glass blocks are developed, fixed and stained.

a wire loop, 2.5 cm in diameter, made of platinum wire or vinyl-coated iron wire into the solution. 3) After air-drying horizontally for 1 min, when the emulsion film is gelled but still wet, the film is applied to the grids on the glass block horizontally (Figure 2A). The glass block is warmed at 28°C for 1 h to dry the emulsion. 4) For exposure, several glass blocks are attached to one side of a microscope slide with double-coated Scotch tape (Figure 2B). 5) Control emulsion films should be checked by electron microscopy before exposure. 6) Several glass slides carrying several glass blocks are placed in a black light-tight plastic slide box containing a desiccant (silica gel), and the top is sealed with black tape. The slide box is kept in a refrigerator at 4°C for exposure. 7) After an appropriate exposure time, the glass slides carrying glass blocks with grid meshes are processed for development, then stopped in a stop bath, fixed in a fixer and stained with lead citrate solution for electron staining.

Concerning the development of the emulsions, when a conventional MQ-developer such as D-19 is used, long spiral silver grains are formed. In order to obtain smaller silver grains, phenidon developer after gold latensification (G-L) is recommended (Figures 3-8). We prefer the following procedure (1,62).

1) The glass slides carrying the grid meshes are first soaked in distilled water in a staining jar for 10 s, and then 2) soaked in G-L solution (0.2 ml 2% aqueous gold chloride solution, 0.05 g potassium thiocyanate, 0.06 g potassium bromide, 100 ml distilled water) for latensification at 16°C for 30 s. 3) The slides are then rinsed in distilled water for 10 s, and 4) soaked in phenidon developer (1.5 g ascorbic acid, 0.25 g phenidon, 0.4 g potassium bromide, 1.3 g potassium carbonate, 20 g sodium sulfite anhydrous, 4.0 g potassium thiocyanate, 100 ml distilled water) in a water bath at 16°C for 60 s for development. 5) They are then soaked in a stopper solution (2% aqueous acetic acid solution) for 10 s, 6) fixed in a fixer (30% aqueous sodium thiosulfate solution) for 5 min, with 2 changes, and 7) rinsed in distilled water for 5 min, with 3 changes. 8) The sections are stained in lead citrate solution (63) for 3 min, and 9) rinsed in distilled water for a few minutes. 10) Finally the grids are carefully removed from the glass blocks with a forceps, placed on filter paper in a Petri dish and dried in an incubator at 37°C for 1 h. 11) The specimens are coated with a 10-nm thick carbon layer in a vacuum coater before electron microscopy.

2.3.2.3. Dry-mounting procedure

Both cryo-sectioned and freeze-dried specimens and freeze-dried or freeze-substituted and embedded specimens should be coated with dry radioautographic emulsions without using any water. The procedure is designated as dry-mounting radioautography. Two types of procedures are used for dry-mounting radioautography, i.e., light microscopic and electron microscopic procedures.

2.3.2.3.1. Light microscopic dry-mounting procedure

Historically, various procedures have been employed for light microscopic dry-mounting radioautography as described previously (24,32-37). Since the first application of cryostat sections to precoated slides at very low temperature by Appleton (24), many authors have recommended this technique for light microscopy. However, these procedures are highly complicated in terms of treatment of both specimens and emulsions. We first used dry-films produced with a large wire loop which were air-dried and applied to cryostat sections placed on glass slides (23). We believe that this method is the most convenient one. The procedure is as follows.

1) Cryostat sections are picked up onto glass slides and dried. Dry epoxy resin sections are expanded over the slides with a

drop of ethylene glycol without using any water. 2) Radioautographic emulsion is diluted with an equal part of distilled water at 45°C. We use Konica NR-M2 emulsion from Konica but any other emulsion such as Kodak can be used. Ten ml of diluted emulsion is added to 0.2 ml of a 2% aqueous solution of dioctyl sodium sulfosuccinate (a surfactant) in order to prevent the emulsion film from bursting (14). 3) A thin film of emulsion is obtained by dipping a wire loop, 2.5 cm in diameter, made of platinum wire or vinyl-coated iron wire and attached with Scotch tape to a glass slide as a handle. 4) The handle is set horizontally on a flat surface for air-drying. 5) After air-drying for 1-2 min, when the center of the emulsion film is gelled and dried and transparent but the peripheral zone is still wet and opaque, the film is applied to the slide horizontally. 6) The glass slide is kept in a Petri dish and warmed at 28°C in an incubator for 1 h for drying the emulsion. 7) Several glass slides are placed in a black light-tight plastic slide box containing desiccant (silica gel), and the top is sealed with black tape. The slide box is kept in a refrigerator at 4°C for exposure. 8) After an appropriate exposure time, the glass slides are processed for development, then stopped in a stop bath, fixed in a fixer and stained with toluidine blue solution. 9) Control tissues should be fixed with chemical fixative, dehydrated, embedded, wet-sectioned and wet-mounted by conventional dipping procedures.

2.3.2.3.2. Electron microscope dry-mounting procedure

For tissues fixed by precipitation fixation, ultrathin Epon sectioning and radioautography can be carried out according to the routine wet-mounting procedures for demonstrating soluble compounds. However, when the tissues are fixed by rapid freezing and freeze-dried or freeze-substituted, they are dry-sectioned and have to be radioautographed by the dry-mounting procedure (17,18). The grids carrying dry sections (either freeze-dried or freeze-substituted Epon-embedded sections or freeze-sectioned and freeze-dried) are coated with a 5-10-nm thick carbon layer before emulsion application. They are then placed on a grid holder made of a glass slide (25 mm x 75 mm) and 3 glass rods (3 mm in diameter and 10 mm in length). The routine procedures for dry-mounting are as follows.

1) The radioautographic emulsion is diluted 1:10 with distilled water at 45°C in a dark room. 2) Ten ml of the diluted emulsion is added to 0.2 ml of 2% aqueous solution of dioctyl sodium sulfosuccinate and maintained at 45°C in a thermobath for several minutes to complete mixing. Dioctyl sodium sulfosuccinate, a surface activating agent, is used to prevent the emulsion films from bursting while they are being air dried (17,23). We use Konica NR-H2 emulsion. Other emulsions for electron microscopic radioautography such as Kodak NTB or Ilford L4 could also be used. The procedures are as follows. 3) A thin film of the emulsion thus prepared is obtained by dipping a platinum wire loop, about 1 cm in diameter, into the emulsion (17). 4) Instead of a small platinum wire loop, a large vinyl-coated iron wire loop, 2.5 cm in diameter, can also be used (1,61). 5) The handle of the wire loop is set on a flat surface for air drying (for 1-2 min). 6) The best condition for applying the film to the grid is in such a way that the peripheral zone of the film appears gelled but wet (opaque) while the central zone is gelled and almost dry, but still transparent. The films are almost 100% air-dried without breaking by using the dioctyl sodium sulfosuccinate. Without this agent, the films will burst most of the time (23). 7) The dried films are then applied to the grids on the holders like quoits and 8) the grids are transferred to Petri dishes and warmed at 37°C for 1 h to help the films adhere to the grids. 9) The grids are kept in a light-tight container with a desiccant, sealed

with black vinyl tape and kept in a refrigerator at 4ºC for exposure.

On the other hand, when several grids are attached to a square glass block, 12.5 mm in length, a large wire loop, 2.5 cm in diameter, can be used as done in the wet-mounting procedure, and several blocks are placed on a slide. They are exposed, developed, fixed and stained simultaneously.

As a control, radioautography should be carried out by conventional procedures for insoluble compounds. The tissues are fixed in 2.5% glutaraldehyde and 1% osmium tetroxide in 0.1 M cacodylate buffer, dehydrated in a graded ethanol series, embedded in Epon, sectioned with water in the knife trough, and wet-mounted with radioautographic emulsion. After an appropriate exposure time, the meshes are transferred to the developer. The author uses gold-latensification and phenidon developer (62). Other types of developer such as Kodak D-19 can also be used. Following processing with the stopper, fixer and several rinses in distilled water, the grids are stained in a lead citrate solution for 3 min for the purpose of both staining and removing the gelatin of the emulsion. We use a lead citrate solution consisting of 10 ml distilled water and 30 mg lead citrate, adjusted to pH 12 with a few drops of 10 N NaOH. A lead citrate solution could also be used according to the method of Reynolds (63). Uranyl staining is usually not necessary.

3. Special radioautographology

Special RAGology consists of applications of general RAGology to various fields of biology and medicine. The applications of RAG to biology and medicine can also be classified into several scientific fields, i.e., cellular and molecular biology, anatomy, histology, embryology, pathology and pharmacology, etc. All the results obtained from such applications should be systematized as a new field of science to be designated as special RAGology in the future.

In this section, the author would like to review briefly the results obtained in cellular and molecular biology, anatomy, histology, embryology, pathology and pharmacology from organ systems of animals and humans in our laboratory.

3.1. Cellular and molecular biology

In cellular and molecular biology, special radioautographology deals with the macromolecular synthesis and intracellular localization of small molecular compounds in living organisms at the cellular and molecular levels.

3.1.1. Macromolecular synthesis

Macromolecular compounds such as nucleic acids (DNA and RNA), proteins, glucides and lipids which are synthesized in cells can be demonstrated at the subcellular level by conventional wet-mounting radioautography in cells and tissues submitted to chemical fixation (64-66).

3.1.1.1. DNA synthesis

DNA is the main component of nucleoproteins and consists of deoxyribose, phosphate, and bases which contain adenine (A), thymine (T), guanine (G) and cytosine (C). [^{3}H]-Thymidine is incorporated into the bases. Light and electron microscopic radioautograms of the gastrointestinal tract of mice and rats labeled with [^{3}H]-thymidine reveal the localization of silver grains over nuclei of the cells during the S-phase of the cell cycle, indicating the sites of DNA synthesis in epithelial cells such as the stomach mucous neck cells and crypt cells in the small and large intestines or glandular cells such as the liver and the pancreas (66). As the results of these studies, the turnover rates of epithelial cells in the intestine were clarified. Cell kinetic studies were extensively

carried out by Leblond and coworkers in the 1960's (67). We have mainly studied the labeling sites and labeling indices as well as cell organelle changes in cell components of parenchymatous digestive organs such as the liver and pancreas, and in esophageal and intestinal epithelial cells of aging mice from the prenatal to the postnatal period by light and electron microscopic radioautography (64,66). We also demonstrated DNA synthesis in some other organ systems such as the respiratory, urogenital, endocrine (Figure 3), circulatory, nervous and sensory systems (12). Extranuclear DNA synthesis in mitochondria or peroxisomes of various cells was also studied under different experimental conditions (68-70).

3.1.1.2. RNA synthesis

RNA is composed of ribose, phosphate and the bases, A, U, G, and C. In order to demonstrate RNA synthesis, [^{3}H]-labeled cytidine was formerly used (71). However, [^{3}H]-cytidine can also be incorporated into DNA although at very low levels, so that demonstration of DNase digestion was necessary to confirm RNA synthesis. In contrast, [^{3}H]-5-uridine was shown to be specifically incorporated into only RNA. Therefore, it has now come to be used routinely for the demonstration of RNA synthesis (1,12,72). When [^{3}H]-uridine is administered to animals, or cultured cells are incubated in a medium containing [^{3}H]-uridine *in vitro* and radioautograms are prepared, silver grains first appear over the chromatin of the nucleus and nucleolus of all the cells within several minutes, then spreading over the cytoplasm within 30 min, showing messenger RNA and ribosomal RNA (Figure 4). We studied quantitative changes of RNA synthesis in the liver and pancreas of aging mice by means of light and electron microscopic radioautography after injection of [^{3}H]-uridine (66). We also demonstrated intramitochondrial RNA synthesis in some cells independently of the nuclei (72,73).

3.1.1.3. Protein synthesis

Proteins consist of polypeptides and the intracellular localization of protein synthesis can be demonstrated by light and electron microscopic radioautography after administration of RI-labeled amino acids such as [^{3}H]-glycine or [^{3}H]-leucine which are incorporated into the endoplasmic reticulum and Golgi apparatus and then transferred to secretory granules or cytoplasmic ground

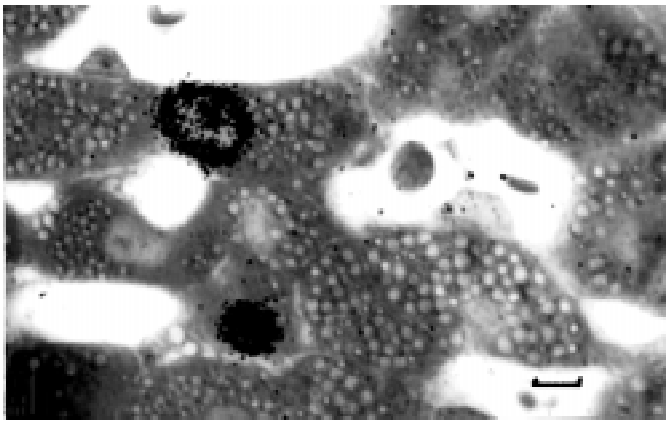

Figure 3 - Light microscopic radioautograms (LMRAG) of the adrenal gland of a 2-week-old mouse injected with [^{3}H]-thymidine, demonstrating DNA synthesis. Two nuclei in the zona fasciculata at the center are labeled with many silver grains. Magnification bar: 5 µm.

Figure 4 - Electron microscopic radioautogram (EMRAG) of HeLa cells cultured *in vitro* in a medium containing [^{3}H]-uridine, demonstrating RNA synthesis. Silver grains are localized over the nucleus (N), nucleolus and cytoplasm. Magnification bar: 1 µm.

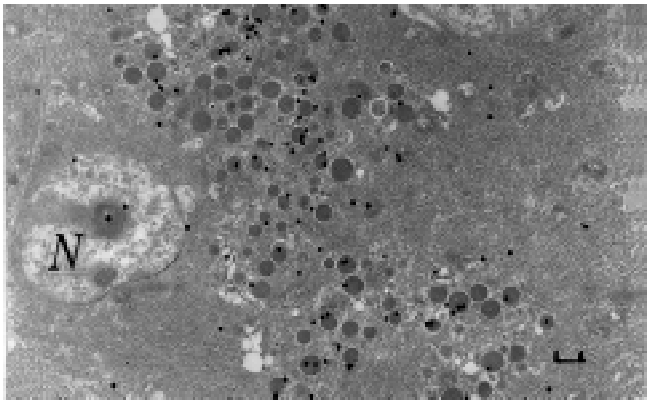

Figure 5 - EMRAG of the pancreas of an adult mouse, 1 month after birth, injected with [^{3}H]-leucine, demonstrating protein synthesis in pancreatic acinar cells. Many silver grains are localized over the endoplasmic reticulum, Golgi apparatus and secretory granules. Magnification bar: 1 µm.

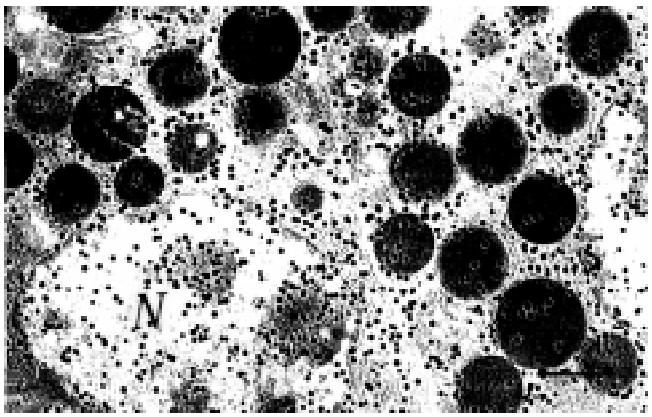

Figure 6 - EMRAG of a 14-day-old mouse injected with [^{3}H]-glucosamine, demonstrating glucide synthesis in a pancreatic acinar cell. Many silver grains are observed over the nucleus, nucleoli, secretory granules and cytoplasmic matrix. Magnification bar: 1 µm.

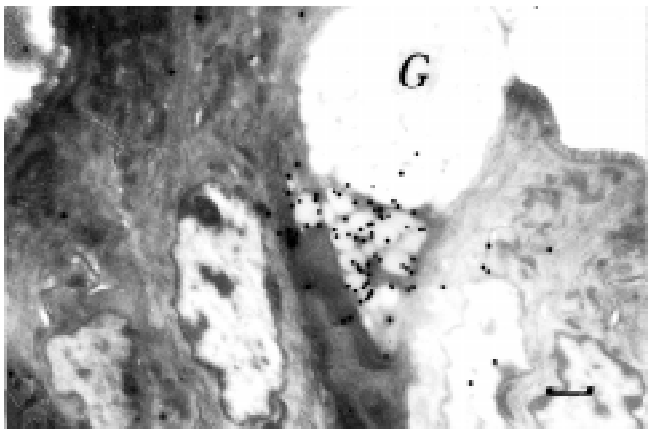

Figure 7 - EMRAG of a goblet cell in the colon of an adult mouse injected with $^{35}SO_4$, demonstrating mucus synthesis. Silver grains are observed over the mucigen granules and the Golgi apparatus. Magnification bar: 1 µm.

substance (Figure 5) and finally discharged outside the cells (64-66). On the other hand, [^{3}H]-proline and [^{3}H]-hydroxyproline are incorporated into endoplasmic reticulum and Golgi apparatus of fibroblasts and accumulate into collagen in the extracellular matrix (74,75).

3.1.1.4. Glucide synthesis

The glucides are classified biochemically into monosaccharides, disaccharides and polysaccharides. Monosaccharides and disaccharides are small water-soluble molecules which cannot be fixed by chemical fixation, but only by cryo-fixation for soluble compounds. Therefore, only polysaccharide synthesis is usually demonstrated by conventional light and electron microscopic radioautography with chemical fixation. Polysaccharides can be classified into simple polysaccharides and complex polysaccharides. Among complex polysaccharides, glycoproteins are composed of proteins and sugar chains, which incorporate [^{3}H]-labeled glucose, galactose, fucose, N-acetyl-glucosamine (Figure 6), etc. (1). On the other hand, mucosubstances or glycosaminoglycans are composed of mucous and proteins, which mainly contain chondroitin sulfate or heparin, and incorporate the radiosulfate $^{35}SO_4$. Therefore, the intracellular localization of mucosubstance synthesis can be demonstrated by light and electron microscopy using $^{35}SO_4$ incorporation (Figure 7). The half-life of radiosulfate is very short, only 87 days, so that experiments should be completed within a few months. We showed incorporation of radiosulfate into the Golgi apparatus and mucigen granules of colonic goblet cells (76).

3.1.1.5. Lipid synthesis

Lipids are esters of high fatty acids and can be classified into simple lipids and compound lipids. The former are composed of

glycerol and fatty acids, while the latter are composed of both lipids and other components such as phosphates, glucides or proteins. In order to demonstrate the intracellular localization of lipid synthesis by light and electron microscopic radioautography, the incorporation of [^{3}H]-glycerol or [^{3}H]-fatty acids was examined (77,78).

3.1.1.6. Gene expression

Recently, gene expression in cells has been demonstrated by *in situ* hybridization. *In situ* hybridization with RI-labeled probes to demonstrate mRNA by light and electron microscopic radioautography has been frequently used. We have demonstrated gene expression of peroxisomal enzymes such as acyl-CoA oxidase mRNA with RI-labeled probes by LM and EMRAG (79-81). Other scientists prefer to use immunostaining rather than radioautography because they believe that the former is easier. However, we prefer radioautography to immunostaining because it has more advantages. The sensitivity of RAG is better than that of immunostaining. The electron density of silver grains is much higher than that of immunochemical deposits when observed by electron microscopy. The intensity of reaction by RAG is quantifiable by grain counting (81) but not by immunostaining. Therefore, this method should be used more often than immunostaining (82).

3.1.2. Small molecular compounds

The small molecular compounds such as precursors of macromolecular compounds, i.e., thymidine, uridine, amino acids, glucosamines, fatty acids or target tracers such as hormones, neurotransmitters, vitamins, inorganic compounds, drugs or toxins cannot be demonstrated by wet-mounting radioautography. They are only demonstrable by means of dry-mounting radioautography (13). We have demonstrated many small molecular compounds in various organs by dry-mounting radioautography (Figure 8), as described in the following sections.

3.2. Anatomy and histology

The results obtained with the applications of various precursors or tracers to all the organ systems should be described according to the conventional order of anatomy and histology of the organs. These results should be included in the histochemistry of the organs (83). The outline of the results obtained from various organ systems in our laboratory will be described briefly.

3.2.1. The organs of movement

3.2.1.1. The bones and joints

DNA synthesis was studied in salamanders of various ages. When salamanders were divided into 8 age groups from larvae to 4, 6, 8, 9,10 weeks and 8, 12 months after hatching and injected with [^{3}H]-thymidine and their forelimbs and hindlimbs were fixed, embedded in Epon, sectioned and radioautographed, the aging changes of DNA synthe-

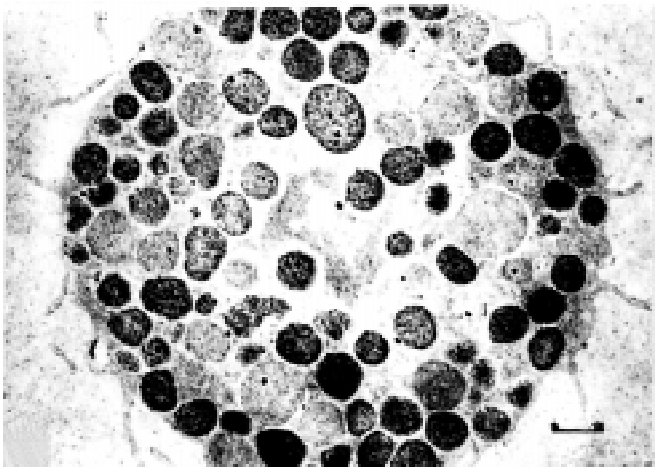

Figure 8 - EMRAG of a mast cell from adult rat peritoneum, incubated in medium containing [^{3}H]-tranilast, a synthetic anti-allergic agent, demonstrating intracellular drug localization. Silver grains are seen over the specific granules in the cytoplasm of the cell. Magnification bar: 1 µm.

sis demonstrated that the labeling indices of chondrocytes in digital bones showed peaks at 4 weeks, then decreased after 6 weeks, reaching 0 at 8 months (84). We also studied DNA, RNA and protein synthesis of normal and rheumatoid synovial membranes surgically obtained from rheumatoid patients and radioautographed by *in vitro* labeling with [^{3}H]-thymidine, [^{3}H]-uridine and [^{3}H]-leucine. No significant differences between normal and rheumatoid tissues were observed (85).

3.2.1.2. The muscular system

The aging changes of DNA synthesis in ddY mouse intercostal muscle from prenatal day 13 through 24 months of postnatal life were studied by [^{3}H]-thymidine radioautography. The labeling indices revealed chronological changes, reaching a peak at embryonic day 13 and decreasing gradually to 0% at 3 months after birth (86). We also studied DNA synthesis in rat thigh muscle when injured and labeled with [^{3}H]-thymidine, demonstrating satellite cell regeneration, as well as DNA synthesis of satellite cells in the muscle of chickens with dystrophy, which will be described in detail in the following pathology section.

As for the incorporation of [^{3}H]-taurine, no difference was found between normal and dystrophy mice by chemical fixation and wet-mounting radioautography. When [^{3}H]-taurine was administered to normal or dystrophy mice and their skeletal muscles were observed in freeze-substituted or freeze-dried specimens followed by dry-mounting radioautography, however, silver grains appeared on the sarcoplasmic reticulum, myofilaments, mitochondria and sarcoplasmic membranes (87,88). More silver grains were observed in normal mice than in dystrophic mice. Only few silver grains were observed in the specimens conventionally fixed with glutaraldehyde and osmium tetroxide followed by wet-mounting radioautography. Based on these results, we conclude that [^{3}H]-taurine is diffusible and is associated with skeletal muscle cells. Taurine is an amino acid which regulates intracellular calcium transport and cell membrane excitability (88).

3.2.2. The digestive system

We have published many papers from our laboratory dealing with the macromolecular synthesis of digestive organs from the oral cavity to the gastrointestinal tract and the digestive glands (66). The outline of the results will be described briefly in the order of systematic anatomy and special histology.

3.2.2.1. The oral cavity

DNA synthesis of mucosal epithelia of the lips and tongue as well as the submandibular glands of aging mice from fetal day 19 to 2 years of postnatal life were studied by LM and EMRAG with [^{3}H]-thymidine. The results showed that the labeling indices of stratified squamous epithelial cells in the oral mucosa increased from perinatal stages to postnatal day 14 and reached steady levels in adults (89), while the indices in the cell types of the submandibular glands increased from the fetal stage to postnatal day 1 and then steadily decreased up to 2 years. Among the cell types in the submandibular glands, the intercalated duct cells were the most frequently labeled and persisted for a longer period. The results suggested that intercalated duct cells are involved in the proliferation of other cell types (90).

3.2.2.2. The esophagus

DNA synthesis in the esophagus of aging mice labeled with [^{3}H]-thymidine was studied by light and electron microscopy (91,92). The labeled cells were mainly found in the basal layer of the esophageal epithelium. Electron microscopy revealed that the nuclei

and nucleoli of labeled cells were larger than those of unlabeled cells, but contained fewer cell organelles (91). The labeling indices in the various age groups showed a peak at 1 day after birth and decreased with aging (92).

3.2.2.3. The stomach

The turnover of fundic glandular cells by [^{3}H]-thymidine radioautography was extensively investigated by Leblond (67). We studied the secretion process in G-cells by EMRAG using [^{3}H]-amino acid. When stomach tissues obtained from Wistar rats were labeled with [^{3}H]-glutamic acid and [^{3}H]-glycine *in vitro* at varying time intervals, silver grains in the radioautograms appeared first over the Golgi zones, then migrated to secretory granules and were stored in the cytoplasm, suggesting a secretory kinetics (93,94). We also studied the mechanism of serum albumin passing through the gastric epithelial cells by EMRAG. When Wistar rat stomach tissues were labeled with [^{132}I]-albumin *in vitro* at varying time intervals, silver grains in the radioautograms appeared over the rough endoplasmic reticulum within 3 min, then moved to the Golgi apparatus within 10 min, and on to secretory granules and into the lumen within 30 min, suggesting the pathway of serum albumin from the blood vessels through the gastric mucous epithelial cells into the gastric lumen (95).

When incorporation of radiosulfate into sulfated complex carbohydrate in rat stomach was studied by labeling with $^{35}SO_4$ *in vivo*, silver grains appeared over the glandular cells of the pyloric gland but not over those of the fundic gland, demonstrating the occurrence of mucus synthesis in the former glands (76).

3.2.2.4. The intestines

DNA synthesis in the small and large intestines of mice was studied by [^{3}H]-thymidine radioautography. The cells labeled with [^{3}H]-thymidine as observed by LMRAG were localized in the crypts of both small and large intestines, a region defined as the proliferative zone. In the colon of mice studied from the fetal stage to 2 years of postnatal life, the labeled cells in the columnar epithelia were frequently found in the perinatal groups from the embryo stage to postnatal day 1. However, the labeling indices became constant from the suckling period to senescence (96). The labeling indices of the cell types in each layer such as columnar epithelial cells, lamina propria, lamina muscularis mucosae, tunica submucosa, inner circular muscle layer, outer longitudinal muscle layer, outer connective tissue and serous membrane of the colon and cecum were examined and it was found that most labeling indices decreased from birth to 2 months except the epithelial cells which kept constant value until senescence (97). Similar results were also obtained for the cecum (98,99).

The synthesis of mucosubstances in goblet cells and in absorptive epithelial cells was studied using $^{35}SO_4$ in the duodenum, jejunum and colon (Figure 8) at varying time intervals (76). The results showed that silver grains over goblet cells in the lower region of the colonic crypt were transferred rapidly from 30 to 180 min, while they were transferred slowly in goblet cells in the upper region of the colonic crypt, leading to the conclusion that the rates of transport and secretion of mucous products of the goblet cells at these two levels in the crypts were different. We also studied the aging changes of [^{3}H]-glucosamine uptake in the mouse ileum and found that the silver grains in the columnar epithelial cells were mainly localized over brush borders and the Golgi region, whereas in the goblet cells they were over the Golgi region and mucous granules. The number of silver grains increased from 6 months up to 2 years due to aging of animals (100).

3.2.2.5. The liver

DNA synthesis of the liver of normal mice was studied by LM and EMRAG using [^{3}H]-thymidine. Normal ddY mice at various prenatal and postnatal ages were injected with [^{3}H]-thymidine which revealed that many silver grains were localized over the nuclei of various cell types constituting the liver, i.e., hepatocytes, sinusoidal endothelial cells, Kupffer cells, Ito's fat-storing cells, bile duct epithelial cells, fibroblasts and hematopoietic cells (101,102). In hematopoietic cells, silver grains were observed over the nuclei of erythroblasts, myeloblasts, lymphoblasts and megakaryocytes. However, most hematopoietic cells disappeared on postnatal day 14. On fetal day 19, the liver tissues consisted chiefly of hepatocytes and hematopoietic cells and no lobular orientation was observed. Lobular formation started on postnatal days 1 and 3. The hepatic lobules were formed on day 9 after birth. During the perinatal period, almost all cell types were labeled with [^{3}H]-thymidine. The percentage of labeled hepatocytes (labeling index) was highest on fetal day 19, and rapidly decreased after birth to day 3. From day 9 to 14, the labeling index gradually decreased, reaching its lowest point at 24 months. When the labeling indices of hepatocytes in 3 hepatic acinar zones were analyzed, they were decreased in the intermediate zone and peripheral zone on days 3 and 9 after birth, whereas they increased in the central zone on day 9, and then completely disappeared from day 14 to 24 months. When the size and number of cell organelles in both labeled and unlabeled hepatocytes on EMRAG were estimated quantitatively by image analysis with an image analyzer, the area of the cytoplasm, nucleus, endoplasmic reticulum, mitochondria as well as the number of mitochondria in the unlabeled hepatocytes was greater than in the labeled cells (103). These data demonstrated that the cell organelles of hepatocytes which synthesized DNA were not well developed as compared to those not synthesizing DNA during postnatal development. In some unlabeled hepatocytes, several silver grains were occasionally observed localized over mitochondria and peroxisomes, as previously reported (68-70). The labeling indices of other cell types such as sinusoidal endothelial cells also showed a decrease from the perinatal period to 24 months (101).

RNA synthesis by the liver of normal mice was studied by [^{3}H]-uridine RAG at the light and electron microscope level. LM and EMRAG showed that silver grains were localized over the nucleoli, nuclear chromatin (both euchromatin and heterochromatin), mitochondria and the rough-surfaced endoplasmic reticulum of hepatocytes as well as other types of cells such as sinusoidal endothelial cells, Kupffer cells, Ito's fat-storing cells, ductal epithelial cells, fibroblasts and hematopoietic cells in the livers at various ages (104). By quantitative analysis, the total number of silver grains in the nucleus, nucleolus and cytoplasm of each hepatocyte increased gradually from fetal day 19, reached a maximum at 14 days of postnatal age, then decreased up to 24 months. The number of silver grains in the nucleolus, when classified into two compartments, (grains over granular components and those over fibrillar components), increased parallelly after birth, reaching their maxima on day 14, and then decreased with aging up to 24 months. However, when the ratios (%) of silver grains over euchromatin and heterochromatin of the nuclei and granular and fibrillar components of the nucleoli were calculated, the ratios remained constant at each aging point.

When [^{3}H]-leucine was injected into mice at various ages silver grains in RAG were observed over all cell types of the liver, i.e., hepatocytes, sinusoidal endothelial cells, ductal epithelial cells, Kupffer cells, Ito's fat-storing cells, fibroblasts and hematopoietic cells (105). In hepatocytes, the number of silver grains in cytoplasm and karyoplasm increased from the perinatal period to 1 month

of postnatal life and decreased with aging up to 24 months. The number of silver grains observed over the cell organelles varied with aging, reaching a maximum at 1 month.

Glucide synthesis was studied by [^{3}H]-glucose incorporation into the mouse liver together with soluble compounds (18,106). Soluble [^{3}H]-glucose, which was demonstrated by cryo-fixation and dry-mounting radioautography, was diffusely localized over the nucleus, all cell organelles and the cytoplasmic ground substance of hepatocytes. By conventional chemical fixation and wet-mounting radioautography, however, silver grains were localized only over glycogen granules, endoplasmic reticulum and Golgi apparatus, a fact demonstrating localization of these macromolecules.

We also observed lipid synthesis in the liver using [^{3}H]-glycerol (18). When adult mice were injected with [^{3}H]-glycerol and the livers were cryo-fixed at -196ºC, freeze-substituted, embedded in epoxy resin, dry-sectioned, and prepared for dry-mounting radioautography, many silver grains appeared diffusely over the nuclei and cytoplasm showing soluble glycerol. However, when the same liver tissues were fixed chemically in buffered glutaraldehyde and osmium tetroxide and radioautographed by conventional wet-mounting procedures, very few silver grains were observed over the endoplasmic reticulum and lipid droplets, demonstrating macromolecular lipid synthesis (18).

3.2.2.6. The pancreas

DNA synthesis in the mouse pancreas was studied by LM and EMRAG using [^{3}H]-thymidine. The nuclei of pancreatic acinar cells (Figure 6), centro-acinar cells, ductal epithelial cells, and endocrine cells were labeled with [^{3}H]-thymidine. The labeling indices of these cells peaked on day 1 after birth and decreased gradually for 24 months (107). Light and electron microscopic radioautograms of the pancreas of mice injected with [^{3}H]-uridine demonstrated incorporation of [^{3}H]-uridine into exocrine and endocrine cells (108). The silver grains were found more in pancreatic acinar cells than in ductal or centro-acinar cells. Among the acinar cells, the number of silver grains increased after birth to day 14 and then decreased with aging. Quantification of silver grains in the nucleoli, chromatin, and cell body was carried out by X-ray microanalysis, which confirmed the results obtained by visual grain counting (55-57).

Incorporation of [^{3}H]-leucine into endoplasmic reticulum, Golgi apparatus and the secretory granules of pancreatic acinar cells was first demonstrated by Jamieson and Palade (109). We have studied [^{3}H]-glycine incorporation into these cell organelles of mouse pancreatic acinar cells with soluble compounds (18). The quantitative aspects of protein synthesis using [^{3}H]-leucine in regard to aging have also been clarified, showing an increase of silver grain numbers after birth, reaching a peak from 2 weeks to 2 months (Figure 5) and decreasing for up to 2 years (110).

As for glucide synthesis, we studied incorporation of [^{3}H]-glucosamine into the glycoproteins of the pancreas of aging mice at various ages by LM and EMRAG (111). When perinatal baby mice received [^{3}H]-glucosamine injections and the pancreatic tissues were radioautographed, silver grains were observed over exocrine and endocrine pancreatic cells. However, these silver grains were few in number. When juvenile mice at the age of 14 days after birth were examined, many silver grains appeared over the exocrine pancreatic acinar cells (Figure 6), with fewer silver grains observed over endocrine pancreatic cells and ductal epithelial cells. The grains in the exocrine pancreatic acinar cells were localized over the nucleus, endoplasmic reticulum, Golgi apparatus and secretory granules, demonstrating glycoprotein synthesis. Adult mice at 1 or 6 months of age and senile mice at 12 or 24 months

showed very few silver grains on radioautograms. Thus, glucide synthesis in the pancreas of mice revealed quantitative changes, i.e., an increase and a decrease of [^{3}H]-glucosamine incorporation with aging.

The lipid synthesis of mouse pancreas was studied by [^{3}H]-glycerol incorporation. When several litters of ddY mice were injected with [^{3}H]-glycerol on fetal day 19, postnatal days 1, 3, 7, and 14, and postnatal months 1, 2, 6 up to 12 months, and the pancreases were prepared for LM and EMRAG, silver grains were observed in both exocrine and endocrine cells at all ages (77,78). In perinatal animals from fetal day 19 to postnatal days 1, 3, and 7, cell organelles were not well developed in exocrine and endocrine cells and the number of silver grains was very low. In 14-day-old juvenile animals, cell organelles such as endoplasmic reticulum, Golgi apparatus, mitochondria and secretory granules were well developed and many silver grains were observed over these organelles and nuclei in both exocrine and endocrine cells. The number of silver grains was higher in exocrine than in endocrine cells. In adult animals aged 1, 2 and 6 months, the number of silver grains remained constant. In 12-month-old senescent animals, silver grains were fewer than in younger animals. The number of silver grains expressed the degree of lipid synthesis, which increased from the perinatal to the adult period and decreased to senescence.

3.2.3. The respiratory system

In the respiratory organs, we have studied macromolecular synthesis in the tracheae and the lungs of mice.

3.2.3.1. The trachea

The changes of DNA synthesis of tracheal cells in aging mice were studied by LM and EMRAG (112). The tracheae of 8 groups of mice from fetal day 18 to 2 years after birth were examined. The results demonstrated that DNA synthesis and morphology of tracheal cells in the mouse tracheae changed with aging. The radioautograms revealed that DNA synthesis in nonciliated and basal cells reached a maximum on fetal day 18, then decreasing from 3 days of postnatal life. The activity of DNA synthesis of ciliated cells was observed but very low in the fetal stage. Ciliated cells cannot synthesize DNA or proliferate in the postnatal stage. They are supposed to be derived by the division and transformation of basal cells. On the other hand, DNA synthesis of chondrocytes was the highest on embryonic day 18, and rapidly declined on postnatal day 3. The chondrocytes lost the ability of synthesizing DNA at 2 months after birth. DNA synthesis of other cells (including fibroblasts, smooth muscle and glandular cells) was highest on fetal day 18 and fell markedly on the third day after birth, decreasing progressively with aging. The incorporation of $^{35}SO_4$ was also studied in the trachea of aging mice. Many silver grains were observed over the chondrocytes and extracellular matrix of the tracheal cartilage in fetal and newborn mice. The numbers of silver grains were highest at 2 weeks after birth and decreased rapidly after 1 month (113).

3.2.3.2. The lung

DNA synthesis of mouse lung was studied by LM and EMRAG (114,115). The lung tissues of aging ddY mice were labeled *in vitro* with [^{3}H]-thymidine and analyzed. As a result, the cell types of the lung, i.e., cuboidal epithelial cells (type 1 epithelial cells), interstitial cells and endothelial cells, showed different labeling indices. The labeling indices of cuboidal epithelial cells (47%), interstitial cells (38%), and endothelial cells (29%) were found to peak on fetal day 18 and postnatal day 1. Then, a second peak appeared on postnatal day 3, after which the index decreased with aging. The aging

changes of DNA synthesis in the lungs of salamanders from larvae (2 months after fertilization), juveniles (1 month), adults (10 and 12 months after metamorphosis) to senescence (5 years) were studied by LMRAG using [^{3}H]-thymidine (116). The result showed that the labeling indices in the ciliated cells and mucous cells in the superficial layer of young animals were higher than those of the basal cells and were decreased in adults, demonstrating aging changes in salamanders. Experiments involving [^{3}H]-thymidine inhalation by means of a nebulizer into the lungs of 1-week-old mice were also carried out. After 45 min of inhalation, the lung tissues were taken out and processed by either rapid-freezing and freeze-substitution for dry-mounting radioautography or conventional chemical fixation for wet-mounting radioautography. By wet-mounting RAG silver grains were observed in the nuclei of a few alveolar type 2 cells and interstitial cells, demonstrating DNA synthesis. By dry-mounting RAG numerous silver grains were located diffusely over all the epithelial cells and interstitial cells, demonstrating soluble compounds (117).

When the lung tissue of mice were labeled with [^{3}H]-uridine, RNA synthesis was observed in all cells of the lung at various ages (118). The number of silver grains changed with aging. The grain counts in type 1 epithelial cells increased from the 1st day after birth and reached a peak at 1 week, while the counts in type 2 epithelial cells and interstitial cells increased from embryonic day 16 and reached peaks at 1 week after birth, decreasing thereafter with aging.

3.2.4. The urinary system

We studied only the macromolecular synthesis of the kidneys of several groups of aging mice, while the localization of anti-allergic agents was observed in the urinary bladders of rats.

3.2.4.1. The kidney

DNA synthesis by [^{3}H]-thymidine radioautography as well as PCNA/cyclin immunohistochemistry was studied in several groups of aging ddY mice from prenatal day 13 to 1 year of postnatal life (119-122). The labeling indices obtained by LMRAG (119) as well as the PCNA/cyclin positive indices (120) in glomeruli (28 to 32%) and uriniferous tubules (31 to 33%) in the superficial layer were higher than those (10 to 12% and 8 to 16%) in the deeper layer from the late fetal to the suckling period, and then decreased with aging from weaning to senescence. Electron microscopic radioautography revealed the same results (121,122). The numbers of silver grains demonstrating the incorporation of [^{3}H]-uridine into glomeruli (34.6 per cell) and uriniferous tubules (56.4 per cell) were higher in the superficial layer than in the deeper layer (15.6 and 18.6 per cell) on embryonic day 15 and gradually decreased with aging (122). The incorporation of [^{3}H]-glucosamine into the kidney of aging mice demonstrated by light and electron microscopic RAG revealed that the numbers of silver grains in both the glomeruli and uriniferous tubules were lower in the embryonic stage, but increased postnatally and reached peaks at 1 to 2 weeks, decreasing thereafter until senescence (123,124).

3.2.4.2. The urinary bladder

Localization of the anti-allergic agent was studied in the urinary bladder of the rat by LMRAG, as described in the section on pharmacology.

3.2.5. The reproductive system

We studied both male and female genital organs of several groups of aging ddY mice by LM and EMRAG using macromolecular precursors.

3.2.5.1. The male genital organs

The study of DNA, RNA and protein synthesis in aging mouse testis by LM and EMRAG revealed incorporation of [^{3}H]-thymidine, [^{3}H]-uridine and [^{3}H]-leucine into various cells of the seminiferous tubules (125,126). In the embryonic and neonatal stages, myoid cells and Sertoli cells labeled with [^{3}H]-thymidine were frequently observed, whereas from young adulthood to senescence the labeling indices of both cells decreased. However, DNA synthesis of gonocytes started 4 days after birth, and the labeling index of spermatogonia first peaked at 3 weeks and stayed constant until senescence. On the other hand, RNA synthesis and protein synthesis of various cells in the seminiferous tubules were weak during the embryonic and neonatal stages (126). The grain counts with [^{3}H]-uridine and [^{3}H]-leucine increased in adult stages and maintained high levels until senescence (125,126).

3.2.5.2. The female genital organs

We have studied the macromolecular synthesis in the ovary, oviduct and uterus of several litters of ddY mice.

3.2.5.2.1. The ovary

DNA and RNA synthesis in developing virgin mouse ovaries were studied by [^{3}H]-thymidine and [^{3}H]-uridine radioautography. [^{3}H]-Thymidine incorporation was active in all surface epithelial cells, stromal and follicular cells of the ovary between postnatal days 1 and 7 and decreased from day 14, remaining at a lower level until day 60 (127,128), while [^{3}H]-uridine incorporation was active in all surface epithelial cells, stromal and follicular cells of the ovary between postnatal days 1 and 7 and maintained medium levels from day 14 on. Mucosubstance synthesis with radiosulfate, $^{35}SO_4$, was studied in the ovaries of mice during the estrous cycle (129). Four groups of female ddY mice aged 8-10 weeks were subdivided into 4 groups, diestrus, proestrus, estrus and metestrus, according to the vaginal smears. The ovaries were removed, labeled with $^{35}SO_4$ *in vitro* and radioautographed. In all animals, silver grains were localized over the granulosa and theca cells. Almost all compartments of the ovary were labeled. The grain counts per cell changed according to cell cycle. From the results, we concluded that all cells of the ovary incorporated mucosubstances throughout the estrous cycle (129).

3.2.5.2.2. The oviduct

DNA and RNA synthesis in the developing virgin mouse oviduct was studied by [^{3}H]-thymidine and [^{3}H]-uridine radioautography (128,129). DNA synthesis was active in all surface epithelial cells, stromal and smooth muscle cells between postnatal days 1 and 3 and decreased from day 7 to 60, while RNA synthesis was observed in the epithelial and stromal cells at postnatal day 1, increasing to days 7 and 14 and then decreasing to day 60 (129).

3.2.5.2.3. The uterus

DNA synthesis of the uterine epithelium, stroma and smooth muscle cells was active on days 1 and 3 and decreased from day 7 to 60, while RNA synthesis of the uterus increased from day 3 to 14 and decreased from day 30 to 60 (127,128).

3.2.6. The endocrine system

We have studied macromolecular synthesis in adrenal glands and Leydig cells of the testis of mice, as well as mercury chloride incorporation into the thyroid in human patients.

3.2.6.1. The thyroid

Normal human thyroid tissues and thyroid cancer tissues obtained from goiter patients by surgery were labeled *in vitro* with $^{203}HgCl_2$ and processed by both conventional chemically fixed wet-mounting radioautography and freeze-dried dry-mounting radioautography (13,130). Numerous silver grains showing soluble mercury components were found diffusely in thyroid cancer cells but fewer silver grains showing insoluble components were observed in cancer and normal thyroid cells (130). The results showed concentration of hot mercury in the thyroid cancer cells from goiter patients.

3.2.6.2. The adrenal gland

Incorporation of [^{3}H]-thymidine and [^{3}H]-uridine was observed in aging mouse adrenal glands from embryo to newborn, young, and 2-year-old senescent adults by light and electron microscopic radioautography (131, 132). DNA synthesis was found in all zones of the adrenal cortex, i.e., the zona glomerulosa, fasciculata and reticularis of the cortex (Figure 3) as well as the medulla from the immature prenatal stage to mature postnatal senescent ages. The labeling indices in the respective zones showed a maximum during the perinatal stage and then gradually decreased to senescent stages. On EMRAG the cell organelles in the labeled cells were less developed than the unlabeled cells in the same zone at the same aging stage (132). On the other hand, the incorporation of [^{3}H]-uridine was found in all layers of both cortex and medulla. Grain counts revealed that the numbers of silver grains were higher in perinatal animals than in older animals and in the zona glomerulosa than in the zona fasciculata or reticularis, or in the medulla (133).

3.2.6.3. The Leydig cells of the testis

The Leydig cells of the testis of several groups of ddY mice at various ages from fetal life to senescence were studied by LM and EMRAG using [^{3}H]-thymidine, [^{3}H]-uridine and [^{3}H]-leucine (134,135). The indices of DNA synthesis obtained by [^{3}H]-thymidine labeling from perinatal stages to 6 months of postnatal life were low (5-10%) but increased at 9 months and maintained high levels (50-60%) up to 2 years. RNA and protein synthesis calculated by grain counting did not change from the fetal stage throughout the adult stages and did not decrease until senescence (135).

3.2.7. The circulatory system

Among the cardiovascular organs, arteries, some blood cells and the spleen were studied in our laboratory.

3.2.7.1. The artery

In the arteries of rats, the localization of calcium antagonists was studied by conventional wet-mounting radioautography and cryo-fixed dry-mounting radioautography. The results will be described in detail in the pharmacology section.

3.2.7.2. The blood cells

DNA, RNA and mucosubstance synthesis of mast cells from Wistar rats (136-138) were studied by [^{3}H]-thymidine, [^{3}H]-uridine and $^{35}SO_4$ radioautography, demonstrating differences in incorporation between normal mast cells (126) and abnormal mastocytoma cells (136,137). Normal rabbit granulocytes were shown by EMRAG and X-ray microanalysis to incorporate $^{35}SO_4$ into the Golgi apparatus and into the gran-

ules, demonstrating glucosaminoglycan synthesis (138).

In studies of drug localization in rat mast cells, we studied tranilast distribution (139,140). The results will be described in detail in the pharmacology section.

3.2.7.3. The spleen

The spleen cells from 6 groups of aging ddY mice at various stages from newborn day 1 to 10 months were examined by light and electron microscopic [^{3}H]-thymidine radioautography combined with acid phosphatase activity (141). DNA synthesis was observed in the nuclei of hematopoietic cells, especially of lymphoblasts and myeloblasts. The aging changes of DNA synthesis as well as acid phosphatase activity were correlated, decreasing from postnatal day 1 and 7 to 10 months. On the contrary, RNA synthesis (142) of hematopoietic cells, especially of the lymphoblasts in the spleens, increased from day 1 to day 14, and then decreased to 10 months after birth.

3.2.8. The nervous system

3.2.8.1. The brain

DNA synthesis was studied in the cerebella of 9 groups of aging mice from embryo stage to 1 year of postnatal age. The labeled nuclei, both the precursors of neurons and glioblasts, were observed in the external granular layer of the cerebella by LMRAG and EMRAG from embryonic day 19 to postnatal day 14 and disappeared within 1 month. The labeling index peaked on postnatal day 3. The endothelial cells of the cerebellar vessels were progressively labeled, reaching a peak 1 week after birth (143). Changes of glucose uptake in the gerbil hippocampus were also studied using [^{3}H]-deoxyglucose by cryo-fixation, freeze-substitution and dry-mounting radioautography under post-ischemic conditions. The results demonstrated that the neurons subjected to ischemia revealed higher uptake of soluble glucose (144).

3.2.9. Sensory system

Among the sensory organs, we mainly studied the eye and, to a lesser extent, the skin.

3.2.9.1. The eye

The synthesis of both DNA and RNA was first studied in the ocular tissues of chick embryos from day 1 to day 14 by LM and EMRAG (145,146). Labeling of cells with [^{3}H]-thymidine was most frequently observed in the posterior region of the optic vesicle of 2-day-old chick embryos and the labeled cells moved from anterior to posterior regions, decreasing from day 3 to day 7 (145,147). On the other hand, the number of silver grains incorporating [^{3}H]-uridine increased from day 1 to day 7 and was higher in the anterior region than in the posterior region (148). DNA and RNA synthesis was also studied in the ocular tissues of aging mice. The ocular tissues obtained from ddY mouse litters at ages varying from fetal day 9, 12, 14, 16, and 19 to postnatal day 1, 3, 7, and 14 were labeled with [^{3}H]-thymidine *in vitro* and radioautographed (149,150). The labeling indices of retina and pigment epithelium were higher in earlier than in later stages, during which they steadily declined. However, the retina and pigment epithelia followed different courses in their changes of labeling indices during embryonic development. In the retina, the labeling indices in the vitreal portions were higher than those in the scleral portions during the earlier stages. However, the indices of scleral portions were higher than those in the vitreal portions in the later stages. Comparing the three regions of the mouse retina, anterior, equatorial and posterior, the labeling indices of the anterior regions were generally higher than those of

the equatorial and posterior regions. In the pigment epithelium, the labeling indices gradually increased in the anterior region, but decreased in the equatorial and posterior regions throughout the developmental stages. These results suggest that the proliferation of both the retina and pigment epithelium in the central region occurred earlier than those in the peripheral regions (149,150). In the juvenile and adult stages, however, the labeled cells were localized in the middle of the bipolar-photoreceptor layer of the retina, where the undifferentiated zone is assumed to be located (151,152). In the corneas of aging mice, the labeled cells were localized in the epithelial cells from prenatal day 19 to 1 year of postnatal life. The labeling index of the corneal epithelial cells reached a peak at 1 month after birth and decreased to 1 year, while the indices of stromal and endothelial cells reached a peak at 3 days after birth and disappeared completely from 1 month to 1 year of postnatal life (153). On the other hand, when the ocular tissues were labeled with [^{3}H]-uridine, silver grains appeared over all cell types at all stages of development and aging. The grain counts increased from prenatal day 9 to postnatal day 1 in the retinal cells, while they increased from prenatal day 12 to postnatal day 7 in the pigment epithelial cells (154).

When protein synthesis was determined in the retina of aging mice by [^{3}H]-leucine incorporation, the number of silver grains in bipolar cells and photoreceptor cells was found to be most intense during embryonic stage and the early postnatal days. The peak was 1 day after birth and decreased from 14 days to 1 year after birth (155).

On the other hand, glycoprotein synthesis determined by [^{3}H]-glucosamine radioautography showed changes of incorporation in the cornea. Silver grains were located in the epithelial cells, the stromal fibroblasts and the endothelial cells from prenatal day 19 to 6 months of postnatal life. No silver grains were observed in the lamina limitans anterior (Bowman's membrane) or the lamina limitans posterior (Descemet's membrane). Grain density was more intense in the endothelial cells of prenatal day 19 animals, but even more intense in the epithelial cells of animals at days 1 and 3 and at 1 week of postnatal life. Glycoprotein synthesis in the various cell types of the mouse cornea changed with animal aging (156).

3.2.9.2. The skin

The DNA synthesis of aging salamander larvae was studied by LMRAG. When 8 groups of salamander from larvae to 4, 6, 8, 9, 10 weeks and 8, 12 months after hatching were injected with [^{3}H]-thymidine and the skins from both the forelimbs and hindlimbs were removed and radioautographed, the labeling indices of epidermal cells increased from 4 weeks to 6 weeks and decreased from 8 weeks on, reaching 0 at 8 months, demonstrating an increase and decrease of DNA synthesis with skin aging (84).

3.3. Embryology

The special radioautographology procedures used in embryology consist of application of radioautography to gametogenesis, blastogenesis and organogenesis. Among these studies, gametogenesis of the male and female genital organs was described in the previous sections (3.2.5.1 and 3.2.5.2).

In order to detect the changes in DNA, RNA and protein synthesis in the mouse endometrium during implantation, the ovulation of female BALB/c mice was controlled with pregnant mare serum gonadotropin and human chorionic gonadotropin, and pregnant female mice were ovariectomized on the 4th day of pregnancy (157-159). A delayed implantation state was maintained for 48 h and after 0 to 18 h of estrogen supply, [^{3}H]-thymidine, [^{3}H]-uridine and [^{3}H]-leucine were injected. The three regions of the endometrium, i.e., the interim-

plantation site, and the antimesometrial and mesometrial sides of the implantation site were processed for LM and EMRAG. The cells labeled with [^{3}H]-thymidine increased after the nidatory effects of estradiol in the stromal cells around the blastocyst, but not in the epithelial cells (157). The cells labeled with [^{3}H]-uridine (148) and [^{3}H]-leucine (159) increased, reaching a peak at 6 h after estrogen induction in both the stromal and epithelial cells on the antimesometrial side. The results suggested that the presence of the blastocyst in the uterine lumen induced selective changes in the behavior of endometrial cells after the nidatory effect of estradiol, showing the changes of DNA, RNA and protein synthesis.

On the other hand, collagen synthesis in the mouse decidual cells was studied by LM and EMRAG using [^{3}H]-proline. Silver grains were localized over the endoplasmic reticulum and Golgi apparatus of fibroblasts and accumulated over collagen fibrils in the extracellular matrix. The results suggested that the decidual cells produced collagen in the matrix (74,75).

The changes in macromolecular synthesis, DNA, RNA, proteins, glucides and lipids during the genesis of various organs of ddY mice were described as perinatal changes in the previous histology chapter. In lower vertebrates, cell proliferation and migration of scleroblasts and their precursor cells during ethisterone-induced anal-fin process formation of the medaka, *Orizias latipes*, were studied by LMRAG (160).

3.4. Pathology

The special radioautographology used in pathology deals with the application of radioautography to pathological changes in various diseases. There are many papers available in the literature and they should be classified according to the pathological description. First of all, the literature can be arranged by such pathological changes as etiology, i.e., the disturbances in the metabolism, the local disturbances in the circulation, proliferation and regeneration of tissues, inflammation, parasites, tumors, and malformations as in general pathology. On the other hand, they can also be arranged according to organ systems as done for anatomy and histology studies. Since we used special radioautographology mainly for normal anatomy and histology studies, we have not published so many papers. Therefore, some of them will be arranged according to the order of etiology as follows.

3.4.1. Disturbances in metabolism

In the thigh muscles of dystrophy chickens, [^{3}H]-thymidine was incorporated into the satellite cells by LM (161) and EMRAG (162), demonstrating the regeneration of these cells, which cannot be observed in normal muscles. With respect to the incorporation of [^{3}H]-taurine, however, no difference was found between normal and dystrophy mice by chemical fixation and wet-mounting radioautography (87). When [^{3}H]-taurine was administered to normal or dystrophy mice (518 kBq/g body weight) and their skeletal muscles were observed in freeze-substituted or freeze-dried specimens followed by dry-mounting radioautography, silver grains appeared on sarcoplasmic reticulum, myofilaments, mitochondria and sarcoplasmic membranes (88), showing soluble compounds. By this method, more silver grains were observed in normal mice than in dystrophy mice. In contrast, only few silver grains were observed in the specimens submitted to conventional glutaraldehyde and osmium tetroxide fixation followed by wet-mounting radioautography (88).

3.4.2. Proliferation and regeneration

When Wistar rat thigh muscles were injured and labeled with [^{3}H]-thymidine, satellite cells were labeled, showing that the re-

generating muscle fibers originated from satellite cells (163).

3.4.3. Inflammation

Experimental studies to clarify the pathogenesis of experimental pancreatitis were carried out by means of LM and EMRAG. Several male Wistar rats were treated with daily DL-ethionine injections for 2 days or for 1 month to cause acute and chronic experimental ethionine pancreatitis. Both normal and experimental pancreatitis animals were then injected with [^{3}H]-ethionine and the pancreatic tissues were fixed and processed for LM and EMRAG 5 or 10 min after injection (164). Many more silver grains were observed over the secretory granules and the lumen of the exocrine pancreatic tissues of pancreatitis animals than normal animals, suggesting that the pathogenesis of ethionine-induced pancreatitis is due to the rapid intracellular transport of ethionine (164).

On the other hand, another group of several male Wistar rats were fed 20% ethanol for 3 months to cause alcoholic pancreatitis. Both the normal and experimental pancreatitis animals were then injected with [^{3}H]-leucine and the pancreatic tissues were fixed and processed for LM and EMRAG 5 to 60 min after injection (165). As a result, fewer silver grains were observed over the secretory granules and the lumen of the exocrine pancreatic tissues of pancreatitis animals than normal animals, suggesting lower protein synthesis in the animals with alcohol-induced pancreatitis (165).

3.4.4. Tumors

Several experiments dealing with nucleic acid synthesis in cancer cells have been performed using LM and EMRAG. The DNA and RNA synthesis in mitochondria of cultured HeLa cells, an established cell line obtained from a carcinoma of the human uterus, labeled with [^{3}H]-thymidine and [^{3}H]-uridine (Figure 4), was demonstrated to be localized over the mitochondrial matrix by EMRAG (72,73). The DNA synthesis of primary cultured myeloma cells obtained from a human myeloma patient was studied by [^{3}H]-thymidine EMRAG (166). From the results, it was demonstrated that the labeled myeloma cells contained poorly developed endoplasmic reticulum as compared with the unlabeled cells, suggesting that immature cells synthesized more DNA than mature cells containing well-developed endoplasmic reticulum (166). DNA, RNA and mucosubstance synthesis by mastocytoma and mast cells from rats (136,137) was studied by [^{3}H]-thymidine, [^{3}H]-uridine and $^{35}SO_4$ RAG, demonstrating that the mastocytoma cells synthesized more DNA, RNA and mucosubstances than normal mast cells (167). On the other hand, when rat ascites hepatoma cells, YS cells, were treated *in vitro* with several carcinogens such as dimethylamine, dimethylnitrosamine, butylbutanolamine, butylurea or butylnitrosourea and processed by EMRAG, no significant difference in [^{3}H]-thymidine and [^{3}H]-uridine incorporation was observed between treated and untreated groups (168).

Human thyroid cancer tissues obtained from goiter patients by surgery were labeled *in vitro* with $^{203}HgCl_2$ and processed by both conventional chemically fixed wet-mounting radioautography and freeze-dried dry-mounting radioautography (130). Numerous silver grains showing soluble component of mercury were found diffusely in thyroid cancer cells but fewer silver grains showing insoluble components were observed in normal and cancer thyroid cells (130). The results supported the clinical findings of a high concentration of hot mercury in the thyroid cancers of goiter patients.

3.5. Pharmacology

The special radioautographology used in pharmacology deals with the organ distribution and intracellular localization of various hormones, vitamins, drugs and toxins. A very extensive literature has been published in this field. The first paper in pharmacology was published by Ullberg (169), who developed the whole body technique in pharmacology and toxicology, and demonstrated for the first time the organ distribution of ^{35}S-penicillin. Since then, extensive literature has been published dealing with the organ distribution of various antibiotics, drugs and hormones by means of whole body RAG. Receptor radioautography has been extensively studied in investigations of hormones such as peptides and steroids. The systematic description of this section should be completed in the future by many pharmacologists who are interested in the use of special radioautographology in pharmacology. We have published only a few papers dealing with this field and we will briefly comment on some of them in this section.

3.5.1. Hormones

Among various hormones available for radioautography, we studied the intracellular localization of [^{3}H]-methyl prednisolone, a synthetic adrenocortical steroid (170). Mouse liver tissue blocks and HeLa cells were labeled *in vitro* with [^{3}H]-methyl prednisolone (Daiichi Pure Chemical Co., Tokyo, Japan; 24.7 GBq/mM, and 3.7 kBq/ml, respectively) resolved in Eagle's MEM supplemented with 10% bovine serum for 1 h. The tissues were quickly frozen in cooled isopentane, freeze-dried and embedded in Epon, or cryo-sectioned and freeze-dried, dry-mounted with Konica NR-H2 emulsion, exposed and developed. In EMRAG, freeze-dried, Epon-embedded sections showed silver grains on the nucleus, nucleolus, endoplasmic reticulum, mitochondria, Golgi apparatus and cytoplasmic matrix of both hepatocytes and HeLa cells. Wet-mounting radioautograms showed fewer grains on the nucleus and cytoplasm. From the results, we concluded that soluble [^{3}H]-methyl prednisolone was distributed diffusely in the cell body, while the insoluble compounds were incorporated into the chromatin, nucleolus, nuclear envelopes, endoplasmic reticulum and mitochondria (170).

3.5.2. Neurotransmitters and inhibitors

The distribution of some of the ophthalmological drugs used for the treatment of glaucoma was examined in the ocular tissues of patients. Bupranolol is a beta-blocking agent widely used in the form of eye drops for glaucoma in the USA and Japan (171). [^{14}C]-Bupranolol (Kaken Co., Tokyo, Japan) was experimentally instilled into the eyes of white rabbits and the ocular tissues were enucleated after 15 and 30 min and cryo-fixed in liquid nitrogen and the frozen tissues were cryo-sectioned and either freeze-dried or thaw-mounted onto glass slides, followed by either dry-mounting or wet-mounting LMRAG. By dry-mounting RAG, silver grains appeared intensely in the conjunctival and corneal epithelia at 15 min, with a later decrease in these tissues and an increase in the ciliary bodies at 30 min. These results demonstrate that bupranolol penetrated the conjunctiva and cornea and accumulated in the ciliary bodies (171).

Befunolol is a beta-blocking agent synthesized by Kaken Co., Tokyo, Japan, whose chemical structure is 2-acetyl-7(2-hydroxy-3-isopropylamino-propoxy) benzofuran hydrochloride. The agent was labeled with [^{3}H] and used for LM and EMRAG (172,173). The ocular tissues of chickens were removed, cut into small pieces and labeled with [^{3}H]-befunolol in Eagle's MEM (3.7 MBq/ml) in a CO_2 incubator for 30 to 60 min. The tissues were cryo-fixed in liquid nitrogen and some of them were dry-sectioned, and some were

freeze-dried or freeze-substituted and embedded in Epon, dry-sectioned and dry-mounted. Some other tissues were chemically fixed, embedded and wet-mounted. Dry-mounting EM radioautograms revealed that many silver grains were found over the melanosomes of the pigmented cells, demonstrating soluble compounds. In contrast, only few silver grains were found over the melanosomes of the pigmented cells of the iris and the ciliary bodies by conventional wet-mounting EMRAG. Soluble [^{3}H]-befunolol was found to accumulate specifically over the melanosomes of the pigmented cells, a result well correlated with the clinical findings.

3.5.3. Anti-allergic agents

One of the synthetic anti-allergic agents, tranilast (synthesized by Kissei Pharmaceutical Co., Matsumoto, Japan) was extensively studied in various organs by LM and EMRAG in our laboratory. Its chemical structure is N-(3, 4-dimethoxycinnamoyl) anthranilic acid, and the agent was labeled with [^{3}H] by NEN, Boston, MA, USA (129,130). When mast cells were collected from Wistar rat peritoneal fluid and labeled *in vitro* for 60 min in PBS containing [^{3}H]-tranilast (3.7 MBq/ml) and chemically fixed and radioautographed by wet-mounting, LM and EMRAG showed accumulation of silver grains over mast cell granules (Figure 8), suggesting the inhibition of degranulation of mast cells for the anti-allergic reaction (139,140).

When the livers of Wistar rats orally treated with [^{3}H]-tranilast were observed by LMRAG, many silver grains were seen over the hepatocyte nuclei and cytoplasm. The grain counts reached a maximum at 3 h after administration, suggesting the occurrence of a metabolic process in the liver (174). Intracellular localization of a peroxisome proliferator, [^{14}C]-labeled bezafibrate was also demonstrated in cultured rat hepatocytes by LM and EMRAG (166,175). About 90% of all the silver grains were localized over the cytoplasm. In EMRAG of whole mount cultured cells, silver grains were localized on the cytoplasmic matrix especially over the endoplasmic reticulum (176). The results showed that the receptors of the peroxisome proliferator were associated with the endoplasmic reticulum (176).

The urinary bladders of rats were investigated by LMRAG after oral administration of [^{3}H]-tranilast. It was found that this agent specifically localized over the transitional epithelial cells and endothelial cells of the veins in the mucosa for a long time, suggesting a relationship with the histopathology of the cystitis observed clinically after the administration of the drug in human patients (177).

3.5.4. Various antagonists

We were asked to collaborate from other research institutions and pharmaceutical companies in order to specify the sites of actions of various kinds of newly developed drugs by localizing the RI-labeled agents using dry-mounting RAG. Some of the results obtained from such collaborative studies treating mainly various antagonists shall be summarized briefly.

3.5.4.1. Anti-metabolic agents

A synthetic compound named W-7, produced by Banyu Pharmaceutical Co., Tokyo, Japan, was found to cause relaxation of vascular smooth muscle, inhibit several Ca^{2+}-calmodulin-dependent enzymes and also inhibit cell proliferation (178). Its chemical structure is N-(6-aminohexyl)-5-chloro-1-naphthylenesulfonamide, which was labeled with [^{3}H] and used for LM and EMRAG. An established cell line from Chinese hamster ovary cells (CHO-K1) was cultured *in vitro* in Ham's F12 medium containing [^{3}H]-labeled W-7 (10 μCi/ml) for 1 h. The cells were collected and fixed by either cryo-

fixation using liquid nitrogen or chemical fixation using various chemical fixatives such as glutaraldehyde, paraformaldehyde and osmium tetroxide, and processed for LM and EMRAG. [^{3}H]-labeled W-7 was demonstrated in the cytoplasmic matrix of CHO cells by glutaraldehyde fixation as well as by cryo-fixation (179).

3.5.4.2. Antihypertensive agents

Many antihypertensive drugs have been recently synthesized and tested in many countries. Among them, one of the new 1,4-dihydropyridine calcium antagonists, benidipine hydrochloride, named Coniel, produced by Kyowa Hakko Kogyo Co., Tokyo, Japan, was studied by LM and EMRAG.

Benidipine hydrochloride was synthesized at the Research Laboratories, Kyowa Hakko Kogyo Co., Shizuoka, Japan and labeled with [^{3}H] by Amersham International, UK, as [^{3}H]-benidipine hydrochloride, while [^{3}H]-nitrendipine was purchased from New England Nuclear, Boston, MA, USA. The animals used were male adult spontaneously hypertensive rats (SHR). The mesenteric arteries were removed and labeled *in vitro* in Eagle's MEM containing either [^{3}H]-benidipine hydrochloride or [^{3}H]-nitrendipine (100 μCi/ml) for 10-30 min, fixed by cryo-fixation in liquid nitrogen or chemical fixation in buffered glutaraldehyde and osmium tetroxide, and processed for either dry-mounting or wet-mounting LM and EMRAG. The results showed that the silver grains related to both drugs were mainly localized over the plasma membranes and the cytoplasm of the smooth muscle cells in the tunica media of the mesenteric arteries, suggesting the presence of the pharmacologically active sites of these drugs (180).

3.5.4.3. Anti-thrombotic agent

One of the new anti-thrombotic agents, cilostazol, 6-[4-(1-cyclohexyl-1H-tetrazol-5yl)butoxy]-3,4-dihydro-2(1H)-quinolinone, is a new specific inhibitor of cyclic AMP phosphodiesterase and was found to have an inhibitory action on platelet aggregation. It was synthesized by Otsuka Pharmaceutical Co., Tokushima, Japan, and labeled with [^{3}H] by Amersham International. The intracellular localization of this agent was studied by LM and EMRAG. Chinese hamster ovary cells were cultured in Ham's F12 medium containing [^{3}H]-cilostazol (10 μCi/ml) for 1 h, fixed in glutaraldehyde and osmium tetroxide, and radioautographed for LM and EMRAG. Many silver grains appeared over the cytoplasmic matrix and cell membranes. This localization suggested the site of action of this drug to be the cytoplasmic matrix (181).

4. Concluding remarks

The methods we have developed in our laboratory to demonstrate both soluble and insoluble radioactive compounds by either wet-mounting or dry-mounting procedures at the light and electron microscope level and to quantify macromolecular synthesis or small molecular compounds by preparing many radioautograms at once, were described in detail.

The results from these methods applied to macromolecular synthesis, DNA, RNA, proteins, glucides and lipids in various organs, as well as the results from dry-mounting procedures, demonstrating hormones, inorganic substances and drugs in various organ systems studied in terms of anatomy, pathology and pharmacology were briefly summarized.

The results obtained by these methods include not only three-dimensional structures of the organs but also the four-dimensional features taking the time dimension into account by labeling cells and localizing the sites of incorporation, synthesis and discharge of the labeled compounds in relation to time lapse and animal aging. The recently

developed technologies and the results obtained from their applications to various organs should be systematized as a new field of science designated as radioautographology, in contrast to the mere techniques which should be simply designated as radioautography.

The methodologies are now well developed and completed and should be applicable to any other substances and animal organs or tissues and cells for *in situ* analysis of cellular functions at the cell organelle and molecular levels. These technologies should be designated as general radioautographology. On the other hand, the results obtained from the applications of radioautography to biology and medicine using various kinds of labeled compounds can be classified into several fields, i.e., anatomy, histology, embryology, cellular and molecular biology, pathology and pharmacology. The results obtained from such applications should be systematized as a new field of science designated as special radioautographology. The present author advocates a new concept of "radioautographology". The new science, named radioautographology, consisting of both subdivisions, general radioautographology (technology) and special radioautographology (applications), is expected to develop rapidly in various fields of biological sciences in the future.

References

1. Nagata T (1992). Radiolabeling of soluble and insoluble compounds as demonstrated by light and electron microscopy. In: Wegmann RJ & Wegmann MA (Editors), *Recent Advances in Cellular and Molecular Biology. Vol. 6. Molecular Biology of Pyridines and DNA, Peroxisomes, Organelles and Cell Movements.* Peeters Press, Leuven, Belgium, 9-21.
2. Nagata T (1996). On the terminology of radioautography *vs* autoradiography. *Journal of Histochemistry and Cytochemistry*, 44: 1209.
3. London ES (1904). Etudes sur la valeur physiologique et pathologique de l'emanation du radium. *Archives d'Electricite Medicale et de Physiotherapie du Cancer*, 12: 363-372.
4. Kotzareff A (1922). Photographies des organes par l'émanation du radium ou radiumgraphie (curiegraphie). *Journal* de *Radiologie et d'Electrologie*, 6: 131-133.
5. Lacassagne A & Lattés JS (1924). Méthode autohisto-radiographique pour la detection dans les organes du polonium injecté. *Comptes Rendus de L'Academie des Sciences*, 178: 488-491.
6. Leblond CP (1943). Localization of newly administered iodine in the thyroid gland as indicated by radioiodine. *Journal of Anatomy*, 77: 149-152.
7. Bélanger LF & Leblond CP (1946). A method for locating radioactive elements in tissues by covering histological sections with a photographic emulsion. *Endocrinology*, 39: 386-400.
8. Pelc SR (1947). Autoradiograph technique. *Nature*, 160: 749-750.
9. Joftes DL & Warren S (1955). Simplified liquid emulsion radioautography. *Journal of the Biological Photographic Association*, 23: 145-150.
10. Leblond CP & Messier B (1958). Renewal of chief cells and goblet cells in the small intestine as shown by radioautography after injection of thymidine-^{3}H into mice. *Anatomical Record*, 132: 247-259.
11. Nagata T (1996). Introductory remarks on radioautography workshop: Radioautographology, general and special. *Cellular and Molecular Biology*, 42 (Suppl): S11-S12.
12. Nagata T (Editor) (1994). *Radioautography in Medicine*. Shinshu University Press, Matsumoto, Japan.
13. Nagata T (1994). Electron microscopic radioautography with cryo-fixation and dry-mounting procedure. *Acta Histochemica et Cytochemica*, 27: 471-489.
14. Shimada M & Watanabe M (1994). Recent progress in whole-body radioautography. *Cellular and Molecular Biology*, 41: 39-48.
15. Nagata T (1997). Three-dimensional observation on whole mount cultured cells and thick sections stained with histochemical reactions by high voltage electron microscopy. In: Motta P (Editor), *Recent Advances in Microscopy of Cells, Tissues and Organs*. Antonio Delfino Editore, Roma, 15-22.
16. Nagata T, Shibata O & Omochi S (1961). A new method for radioautographic observation on isolated cells. *Histochemie*, 2: 255-259.
17. Nagata T, Nawa T & Yokota S (1969). A new technique for electron microscopic dry-mounting radioautography of soluble compounds. *Histochemie*, 18: 241-249.
18. Nagata T & Murata F (1977). Electron microscopic dry-mounting radioautography for diffusible compounds by means of ultracryotomy. *Histochemistry*, 54: 75-82.
19. Nagata T & Shimamura K (1958). Radioautographic studies on calcium absorption. I. Calcium absorption in the stomach of rat. *Medical Journal of the Shinshu University*, 3: 83-90.
20. Nagata T & Shimamura K (1959). Radioautographic studies on calcium absorption. II. Calcium absorption in the intestines of rat. *Medical Journal of the Shinshu University*, 4: 1-10.
21. Nagata T & Shimamura K (1959). Radioautographic studies on calcium absorption. III. Distribution of radiocalcium in the liver and the kidney of rat after oral administration. *Medical Journal of the Shinshu University*, 4: 11-18.
22. Mizuhira V, Uchida K, Totsu J & Shindo H (1968). Studies on the absorption of S-benzoylthiamine O-monophosphate (in Japanese). *Vitamins*, 38: 334-346.
23. Nagata T & Nawa T (1966). A modification of dry-mounting technique for radioautog-

raphy of water-soluble compounds. *Histochemie*, 7: 370-371.
24. Appleton TC (1964). Autoradiography of soluble labeled compounds. *Journal of the Royal Microscopic Society*, 83: 277-281.
25. Christensen AK (1971). Frozen thin sections of fresh tissue for electron microscopy, with a description of pancreas and liver. *Journal of Cell Biology*, 51: 772-804.
26. Mizuhira V, Shiihashi M & Futaesaku Y (1981). High-speed electron microscope autoradiographic studies of diffusible compounds. *Journal of Histochemistry and Cytochemistry*, 29: 143-160.
27. Futaesaku Y & Mizuhira V (1986). Negative-staining autoradiography: A new technique for ultracryotomy utilizing an interposed film. *Journal of Histochemistry and Cytochemistry*, 34: 1085-1094.
28. Edwards LC & Udupa KN (1957). Autoradiographic determination of S35 in tissues after injection of methionin-S35 and sodium sulfate-S35. *Journal of Biophysical and Biochemical Cytology*, 3: 757-770.
29. Smitherman TC, Debons AF, Pittman JA & Stephens V (1963). Movement of water-soluble material in Mayer's albumin and a simplified dry-mounting method for autoradiography. *Nature*, 198: 499-500.
30. Miller Jr OL, Stone GE & Prescott DM (1964). Autoradiography of soluble materials. *Journal of Cell Biology*, 23: 654-658.
31. Stirling CE & Kinter WB (1967). High resolution radioautography of galactose-^{3}H accumulation in rings of hamster intestine. *Journal of Cell Biology*, 35: 585-604.
32. Kinter WB, Leape LL & Cohen JJ (1960). Autoradiographic study of Diodrast-I131 transport in *Necturus* kidney. *American Journal of Physiology*, 199: 931-942.
33. Fitzgerald PJ (1961). Dry-mounting autoradiographic technic for intracellular localization of water-soluble compounds in tissue sections. *Laboratory Investigation*, 10: 846-856.
34. Stumpf WE & Roth LJ (1964). Vacuum freeze drying of frozen sections for dry-mounting high resolution autoradiography. *Stain Technology*, 39: 219-223.
35. Stumpf WE & Roth LJ (1966). High resolution autoradiography with dry-mounting freeze-dried frozen sections. Comparative study of six methods using two diffusible compounds, ^{3}H-estradiol and ^{3}H-mesobilirubinogen. *Journal of Histochemistry and Cytochemistry*, 14: 274-287.
36. Stumpf WE & Roth LJ (1969). Autoradiography using dry-mounted freeze-dried sections. In: Roth LJ & Stumpf WE (Editors), *Autoradiography of Diffusible Substances*. Academic Press, New York and London, 69-80.
37. Hammarstrom L, Appelgren L-E & Ullberg S (1965). Improved method for light microscopy autoradiography with isotopes in water-soluble form. *Experimental Cell Research*, 37: 608-613.
38. Rogers AW, Thomas GH & Yates KM (1965). Autoradiographic studies on the distribution of labeled progesterone in the uterus of the rat. *Experimental Cell Research*, 40: 668-673.
39. Bernhard W & Leduc EH (1967). Ultrathin frozen sections. I. Methods and ultrastructural preservation. *Journal of Cell Biology*, 34: 757-771.
40. Tokuyasu K (1973). A technique for ultracryotomy of cell suspensions and tissues. *Journal of Cell Biology*, 57: 551-565.
41. Sakai T, Shimakura S & Sakamoto H (1974). The ultrathin section for low temperature. *Proceedings of the 8th International Congress on Electron Microscopy*, 2: 56-57.
42. Nagata T, Ohno S, Yoshida K & Murata F (1978). A simple picking up device for cryosections. *Science Tools*, 25: 59-60.
43. Altmann R (1890). *Die Elementarorganismen und ihre Beziehungen zur Zelle*. Veit und Co., Leipzig.
44. Gersh I (1932). The Altmann technique for fixation by drying while freezing. *Anatomical Record*, 53: 309-324.
45. Gersh I (1956). The preparation of frozen-dried tissue for electron microscopy. *Journal of Biophysical and Biochemical Cytology*, 2 (Suppl): 37-55.
46. Pearse AGE (1968). *Histochemistry, Theoretical and Applied*. 3rd edn. Vol. I. J & A Churchill Ltd., London, 50-51.
47. Luft JE (1961). Improvements in epoxy resin embedding methods. *Journal of Biophysical and Biochemical Cytology*, 9: 409-414.
48. Nagata T, Murata F, Yoshida K, Ohno S & Iwadare N (1977). Whole mount radioautography of cultured cells as observed by high voltage electron microscopy. *Proceedings of the 5th International Congress on High Voltage and Electron Microscopy*, 347-350.
49. Nagata T (1995). Three-dimensional observation of whole mount cultured cells stained with histochemical reactions by ultrahigh voltage electron microscopy. *Cellular and Molecular Biology*, 41: 783-792.
50. Simpson WL (1941). An experimental analysis of the Altmann technic of freezing drying. *Anatomical Record*, 80: 173-185.
51. Lison L (1960). *Histochimie et Cytochimie Animales, Principles et Methodes*. 3rd edn. Gauthier-Villards, Paris, 532.
52. Trump BF (1969). Autoradiography of diffusible substances. In: Roth LJ & Stumpf WE (Editors), *Autoradiography of Diffusible Substances*. Academic Press, New York and London, 211-240.
53. Van Harrevelt A & Crowell J (1964). Electron microscopy after rapid freezing on a metal surface and substitution fixation. *Anatomical Record*, 149: 381-386.
54. Nagata T (1972). Electron microscopic dry-mounting autoradiography. *Proceedings of the 4th International Congress on Histochemistry and Cytochemistry*, 43-44.
55. Nagata T (1993). Quantitative analysis of histochemical reactions: Image analysis of light and electron microscopic radioautograms. *Acta Histochemica et Cytochemica*, 26: 281-191.
56. Nagata T (1995). Morphometry in anatomy: image analysis on fine structure and histochemical reactions with special reference to radioautography. *Italian Journal of Anatomy and Embryology*, 100 (Suppl 1): 591-605.
57. Nagata T (1991). Electron microscopic radioautography and analytical electron microscopy. *Journal of Clinical Electron Microscopy*, 24: 441-442.
58. Nagata T (1996). Techniques and application of electron microscopic radioautography. *Journal of Electron Microscopy*, 45: 258-274.
59. Nagata T, Shibata S & Nawa T (1967). Simplified methods for mass production of radioautographs. *Acta Anatomica Nipponica*, 42: 162-166.
60. Nagata T (1982). Simple method for mass production of radioautographs. *Cell* (Saibo, in Japanese), 14: 40-50.
61. Yoshida K, Murata F, Ohno S & Nagata T (1978). A modified wire-loop method for quantitative electron microscopic radioautography. *Histochemistry*, 57: 93-96.
62. Murata F, Yoshida K, Ohno S & Nagata T (1979). Electron microscopic radioautography using a combination of phenidone developer and domestic emulsion. *Acta Histochemica et Cytochemica*, 12: 443-450.
63. Reynolds ES (1963). The use of lead citrate at high pH as an electron opaque stain in electron microscopy. *Journal of Cell Biology*, 17: 208-212.
64. Nagata T (1993). Quantitative light and electron microscopic radioautographic studies on macromolecular synthesis in several organs of prenatal and postnatal aging mice. *Chinese Journal of His-*

tochemistry and Cytochemistry, 2: 106-108.
65. Nagata T (1994). Application of electron microscopic radioautography to clinical electron microscopy. *Medical Electron Microscopy*, 27: 191-212.
66. Nagata T (1995). Light and electron microscopic radioautographic studies on macromolecular synthesis in digestive organs of aging mice. *Cellular and Molecular Biology*, 41: 21-38.
67. Leblond CP (1981). The life history of cells in renewing systems. *American Journal of Anatomy*, 160: 113-158.
68. Nagata T, Shibata S & Nawa T (1967). Incorporation of tritiated thymidine into mitochondrial DNA of the liver and kidney cells of chickens and mice in tissue culture. *Histochemie*, 10: 305-308.
69. Nagata T, Ohno S, Yoshida K & Murata F (1982). Nucleic acid synthesis in proliferating peroxisomes of rat liver as revealed by electron microscopical radioautography. *Histochemical Journal*, 14: 197-204.
70. Nagata T, Fujii Y & Usuda N (1982). Demonstration of extranuclear nucleic acid synthesis in mammalian cells under experimental conditions by electron microscopic radioautography. *Proceedings of the 10th International Congress on Electron Microscopy*, 2: 305-306.
71. Nagata T (1967). On the increase of binucleate cells in the ganglion cells of dog small intestine due to experimental ischemia. *Medical Journal of the Shinshu University*, 12: 93-113.
72. Nagata T (1972). Electron microscopic radioautography of intramitochondrial RNA synthesis of HeLa cells in culture. *Histochemie*, 32: 163-170.
73. Nagata T (1972). Quantitative electron microscope radioautography of intramitochondrial nucleic acid synthesis. *Acta Histochemica et Cytochemica*, 5: 201-203.
74. Oliveira SF, Abrahamsohn PA, Nagata T & Zorn TMT (1995). Incorporation of ^{3}H-amino acids by endometrial stromal cells during decidualization in the mouse. A radioautographical study. *Cellular and Molecular Biology*, 41: 107-116.
75. Oliveira SF, Nagata T, Abrahamsohn PA & Zorn TMT (1991). Electron microscopic radioautographic study on the incorporation of ^{3}H-proline by mouse decidual cells. *Cellular and Molecular Biology*, 37: 315-323.
76. Nagata T, Kawahara I, Usuda N, Maruyama M & Ma H (1988). Radioautographic studies on the glycoconjugate synthesis in the gastrointestinal mucosa of the mouse. In: Ohyama M & Muramatsu T (Editors), *Glycoconjugate in Medicine*. Professional Postgraduate Service, Tokyo, 251-256.
77. Nagata T, Usuda N, Maruyama M & Ma H (1988). Electron microscopic radioautographic study on lipid synthesis in perinatal mouse pancreas. *Journal of Clinical Electron Microscopy*, 21: 756-757.
78. Nagata T, Usuda N & Ma H (1990). Electron microscopic radioautography of lipid synthesis in pancreatic cells of aging mice. *Journal of Clinical Electron Microscopy*, 23: 841-842.
79. Usuda N & Nagata T (1992). Electron microscopic radioautography of acyl-CoA mRNA by *in situ* hybridization. *Journal of Clinical Electron Microscopy*, 25: 332-333.
80. Usuda N, Hanai T, Morita T & Nagata T (1992). Radioautographic demonstration of peroxisomal acyl-CoA oxidase mRNA by *in situ* hybridization. In: Wegmann RJ & Wegmann M (Editors), *Recent Advances in Cellular and Molecular Biology*. *Vol. 6. Molecular Biology of Pyridines and DNA, Peroxisomes, Organelles and Cell Movements*. Peeters Press, Leuven, Belgium, 181-184.
81. Usuda N & Nagata T (1995). The immunohistochemical and *in situ* hybridization studies on hepatic peroxisomes. *Acta Histochemica et Cytochemica*, 28: 169-172.
82. Nagata T & Usuda N (1993). *In situ* hybridization by electron microscopy using radioactive probes. *Proceedings of the Histochemical Society 44th Annual Meeting*. *Journal of Histochemistry and Cytochemistry*, 41: 1119 (Abstract).
83. Nagata T (1995). Histochemistry of the organs - Application of histochemistry to anatomy. *Acta Anatomica Nipponica*, 70: 448-471.
84. Kobayashi K, Matsumura K & Nagata T (1995). Aging changes of DNA synthesis in salamander cartilage and skin by microscopic radioautography. *Acta Anatomica Nipponica*, 70: B20 (Abstract).
85. Kobayashi K & Nagata T (1994). Light microscopic radioautographic studies on DNA, RNA and protein synthesis in human synovial membrane of rheumatoid arthritis patients. *Journal of Histochemistry and Cytochemistry*, 42: 982 (Abstract).
86. Hayashi K & Nagata T (1993). Radioautographic study on ^{3}H-thymidine incorporation at different stages of muscle development in aging mice. *Cellular and Molecular Biology*, 39: 553-560.
87. Terauchi A, Mori T, Kanda H, Tsukada M & Nagata T (1988). Radioautographic study of 3H-taurine uptake in mouse skeletal muscle cells. *Journal of Clinical Electron Microscopy*, 21: 627-628.
88. Terauchi A & Nagata T (1993). Observation on incorporation of ^{3}H-taurine in mouse skeletal muscle cells by light and electron microscopic radioautography. *Cellular and Molecular Biology*, 39: 397-404.
89. Watanabe I, Jin C & Nagata T (1997). A light and electron microscopic radioautographic study of the mouse lip mucosa. *Proceedings of the 5th International Symposium on Radioautography,* São Paulo, Brazil (in press).
90. Chen S, Gao F, Kotani A & Nagata T (1995). Age-related changes of male mouse submandibular gland: A morphometric and radioautographic study. *Cellular and Molecular Biology*, 41: 117-124.
91. Duan H, Gao F, Li S, Hayashi K & Nagata T (1992). Aging changes of the fine structure and DNA synthesis of esophageal epithelium in neonatal, adult and old mice. *Journal of Clinical Electron Microscopy*, 25: 452-453.
92. Duan H, Gao F, Li S & Nagata T (1993). Postnatal development and aging of esophageal epithelium in mouse: A light and electron microscopic radioautographic study. *Cellular and Molecular Biology*, 39: 309-316.
93. Sato A, Iida F, Furihara R & Nagata T (1977). Electron microscopic radioautography of rat stomach G-cells by means of 3H-amino acids. *Journal of Clinical Electron Microscopy*, 10: 358-359.
94. Sato A (1978). Quantitative electron microscopic studies on the kinetics of secretory granules in G-cells. *Cell and Tissue Research*, 187: 45-59.
95. Komiyama K, Iida F, Furihara R, Murata F & Nagata T (1978). Electron microscopic radioautographic study on 125I-albumin in rat gastric mucosal epithelia. *Journal of Clinical Electron Microscopy*, 11: 428-429.
96. Morita T, Usuda N, Hanai T & Nagata T (1993). Changes of colon epithelium proliferation due to individual aging with PCNA/cyclin immunostaining comparing with ^{3}H-thymidine radioautography. *Histochemistry*, 101: 13-20.
97. Jin C (1995). Study on DNA synthesis of aging mouse colon by light and electron microscopic radioautography. *Cellular and Molecular Biology*, 41: 255-268.
98. Jin C & Nagata T (1995). Light microscopic radioautographic study on DNA synthesis in cecal epithelial cells of aging mice. *Journal of Histochemistry and Cytochemistry*, 43: 1223-1228.
99. Jin C & Nagata T (1995). Electron microscopic radioautographic study on DNA

synthesis in cecal epithelial cells of aging mice. *Medical Electron Microscopy*, 28: 71-75.
100. Morita T (1993). Radioautographic study on the aging change of ^{3}H-glucosamine uptake in mouse ileum. *Cellular and Molecular Biology*, 39: 875-884.
101. Ma H (1988). Studies on DNA synthesis of aging mice by means of light microscopic radioautography. *Acta Anatomica Nipponica*, 61: 137-147.
102. Ma H & Nagata T (1988). Studies on DNA synthesis of aging mice by means of electron microscopic radioautography. *Journal of Clinical Electron Microscopy*, 21: 715-716.
103. Ma H & Nagata T (1990). Electron microscopic radioautographic studies on DNA synthesis in the hepatocytes of aging mice as observed by image analysis. *Cellular and Molecular Biology*, 36: 73-84.
104. Ma H & Nagata T (1990). Study on RNA synthesis in the livers of aging mice by means of electron microscopic radioautography. *Cellular and Molecular Biology*, 36: 589-600.
105. Ma H, Gao F, Olea MT & Nagata T (1991). Protein synthesis in the livers of aging mice studied by electron microscopic radioautography. *Cellular and Molecular Biology*, 37: 607-615.
106. Nagata T, Ohno S & Murata F (1977). Electron microscopic dry-mounting radioautography for soluble compounds. *Acta Pharmacologica et Toxicologica*, 41: 62-63.
107. Nagata T, Usuda N & Ma H (1984). Electron microscopic radioautography of nucleic acid synthesis in pancreatic acinar cells of prenatal and postnatal aging mice. *Proceedings of the 11th International Congress on Electronic Microscopy*, 3: 2281-2282.
108. Nagata T & Usuda N (1986). Studies on the nucleic acid synthesis in pancreatic acinar cells of aging mice by means of electron microscopic radioautography. *Journal of Clinical Electron Microscopy*, 19: 486-487.
109. Jamieson JD & Palade GE (1967). Intracellular transport of secretory proteins in the pancreatic exocrine cells. *Journal of Cell Biology*, 34: 577-615.
110. Nagata T & Usuda N (1993). Electron microscopic radioautography of protein in pancreatic acinar cells of aging mice. *Acta Histochemica et Cytochemica*, 26: 481-481.
111. Nagata T, Usuda N, Suzawa H & Kanzawa M (1992). Incorporation of ^{3}H-glucosamine into the pancreatic cells of aging mice as demonstrated by electron microscopic radioautography. *Journal of Clinical Electron Microscopy*, 25: 646-647.
112. Sun L, Gao F, Jin C & Nagata T (1996). DNA synthesis in the aging mice tracheae by means of light and electron microscopic radioautography. *Acta Histochemica et Cytochemica*, 30: 211-220.
113. Nagata T, Ohno S, Yamabayashi S, Fujii S & Kawahara I (1980). Radioautographic studies on macromolecular synthesis of various tissues of mice by aging. *Acta Anatomica Nipponica*, 55: 77 (Abstract).
114. Sun L, Gao F, Duan H & Nagata T (1994). Light microscopic radioautography of DNA synthesis in pulmonary cells in aging mice. In: Nagata T (Editor), *Radioautography in Medicine*. Shinshu University Press, Matsumoto, 201-205.
115. Sun L, Gao F, Jin C, Duan H & Nagata T (1995). An electron microscopic radioautographic study on the DNA synthesis of pulmonary tissue cells in aging mice. *Medical Electron Microscopy*, 28: 129-131.
116. Matsumura H, Kobayashi Y, Kobayashi K & Nagata T (1994). Light microscopic radioautographic study of DNA synthesis in the lung of aging salamander, *Hynobius nebulosus*. *Journal of Histochemistry and Cytochemistry*, 42: 1004 (Abstract).
117. Duan H, Gao F, Oguchi K & Nagata T (1994). Light and electron microscopic radioautographic study on the incorporation of 3H-thymidine into the lung by means of a new nebulizer. *Drug Research*, 44: 880-883.
118. Sun L (1995). Age-related changes of RNA synthesis in the lungs of aging mice by light and electron microscopic radioautography. *Cellular and Molecular Biology*, 41: 1061-1072.
119. Hanai T (1993). Light microscopic radioautographic study of DNA synthesis in the kidneys of aging mice. *Cellular and Molecular Biology*, 39: 81-91.
120. Hanai T, Usuda N, Morita T, Shimizu T & Nagata T (1993). Proliferative activity in the kidneys of aging mice evaluated by PCNA/cyclin immunohistochemistry. *Cellular and Molecular Biology*, 39: 181-191.
121. Hanai T & Nagata T (1994). Study on the nucleic acid synthesis in the aging mouse kidney by light and electron microscopic radioautography. In: Nagata T (Editor), *Radioautography in Medicine*. Shinshu University Press, Matsumoto, 209-214.
122. Hanai T & Nagata T (1994). Electron microscopic study on nucleic acid synthesis in perinatal mouse kidney tissue. *Medical Electron Microscopy*, 27: 355-357.
123. Joukura K & Nagata T (1995). Aging changes of ^{3}H-glucosamine incorporation into mouse kidney observed by radioautography. *Acta Histochemica et Cytochemica*, 28: 494 (Abstract).
124. Joukura K (1996). The aging changes of glycoconjugate synthesis in mouse kidney studied by ^{3}H-glucosamine radioautography. *Acta Histochemica et Cytochemica*, 29: 57-63.
125. Gao F (1993). Study on the macromolecular synthesis in aging mouse seminiferous tubules by light and electron microscopic radioautography. *Cellular and Molecular Biology*, 39: 659-672.
126. Gao F, Ma H, Sun L & Nagata T (1994). Electron microscopic radioautographic study on the nucleic acid and protein synthesis in the aging mouse testis. *Medical Electron Microscopy*, 27: 360-362.
127. Li S (1994). Relationship between cellular DNA synthesis, PCNA expression and sex steroid hormone receptor status in the developing mouse ovary, uterus and oviduct. *Histochemistry*, 102: 405-413.
128. Li S & Nagata T (1995). Nucleic acid synthesis in the developing mouse ovary, uterus and oviduct studied by light and electron microscopic radioautography. *Cellular and Molecular Biology*, 41: 185-195.
129. Li S, Gao F, Duan H & Nagata T (1992). Radioautographic study on the uptake of $^{35}SO_4$ in mouse ovary during the estrus cycle. *Journal of Clinical Electron Microscopy*, 25: 709-710.
130. Nagata T, Yoshida K & Murata F (1977). Demonstration of hot and cold mercury in the human thyroid tissues by means of radioautography and chemography. *Acta Pharmacologica et Toxicologica*, 41: 60-61.
131. Ito M (1995). The radioautographic studies on aging change of DNA synthesis and the ultrastructural development of mouse adrenal gland. *Cellular and Molecular Biology*, 42: 14-29.
132. Ito M & Nagata T (1996). Electron microscopic radioautographic studies on DNA synthesis and ultrastructure of aging mouse adrenal gland. *Medical Electron Microscopy*, 29: 145-152.
133. Lian Y, Ito M & Nagata T (1997). Radioautographic study on RNA synthesis in the adrenals of aging mice. *Proceedings*

of the XIV International Symposium on Morphology Sciences, Beijing, China (in press).
134. Gao F, Chen S, Sun L, Kang W, Wang Z & Nagata T (1995). Radioautographic study of the macromolecular synthesis of Leydig cells in aging mouse testis. *Cellular and Molecular Biology*, 41: 145-150.
135. Gao F, Jin C, Ma H, Sun L & Nagata T (1995). Ultrastructural and radioautographic studies on DNA synthesis in Leydig cells of aging mouse testis. *Cellular and Molecular Biology*, 41: 151-160.
136. Murata F, Momose Y, Yoshida K & Nagata T (1977). Incorporation of ^{3}H-thymidine into nuclei of mast cells in adult rat peritoneum. *Shinshu Medical Journal*, 25: 72-77.
137. Murata F, Yoshida K, Ohno S & Nagata T (1978). Ultrastructural and electron microscopic radioautographic study on the mastocytoma cells and mast cells. *Journal of Clinical Electron Microscopy*, 13: 582-583.
138. Murata F, Yoshida K, Ohno S & Nagata T (1979). Mucosubstances of rabbit granulocytes studied by means of electron microscopic radioautography and X-ray microanalysis. *Histochemistry*, 61: 130-150.
139. Nagata T, Nishigaki T & Momose Y (1986). Localization of anti-allergic agent in rat mast cells demonstrated by light and electron microscopic radioautography. *Acta Histochemica et Cytochemica*, 19: 669-683.
140. Nishigaki T, Momose Y & Nagata T (1987). Light microscopic radioautographic study of the localization of anti-allergic agent, tranilast, in rat mast cells. *Histochemical Journal*, 19: 533-536.
141. Olea MT & Nagata T (1992). Simultaneous localization of 3H-thymidine incorporation and acid phosphatase activity in mouse spleen: Electron microscopic radioautography and cytochemistry. *Cellular and Molecular Biology*, 38: 115-122.
142. Olea MT & Nagata T (1992). A radioautographic study on RNA synthesis in aging mouse spleen after ^{3}H-uridine labeling *in vitro*. *Cellular and Molecular Biology*, 38: 399-405.
143. Cui H (1995). Light microscopic radioautographic study on DNA synthesis of nerve cells in the cerebella of aging mice. *Cellular and Molecular Biology*, 41: 1139-1154.
144. Izumiyama K, Kogure K, Kataoka S & Nagata T (1987). Quantitative analysis of glucose after transient ischemia in the gerbil hippocampus by light and electron microscope radioautography. *Brain Research*, 416: 175-179.
145. Gunarso W (1984). Radioautographic studies on the nucleic acid synthesis of the retina of chick embryo. I. Light microscopic radioautography. *Shinshu Medical Journal*, 32: 231-240.
146. Gunarso W (1984). Radioautographic studies on the nucleic acid synthesis of the retina of chick embryo. II. Electron microscopic radioautography. *Shinshu Medical Journal*, 32: 241-248.
147. Gunarso W, Gao F, Cui H, Ma H & Nagata T (1996). A light and electron microscopic radioautographic study on RNA synthesis in the retina of chick embryo. *Acta Histochemica*, 98: 309-322.
148. Gunarso W, Gao F & Nagata T (1997). Development and DNA synthesis in the retina of chick embryo observed by light and electron microscopic radioautography. *Cellular and Molecular Biology*, 43: 189-201.
149. Gao F, Li S, Duan H, Ma H & Nagata T (1992). Electron microscopic radioautography on the DNA synthesis of prenatal and postnatal mice retina after labeled thymidine injection. *Journal of Clinical Electron Microscopy*, 25: 721-722.
150. Gao F, Toriyama K & Nagata T (1992). Light microscopic radioautographic study on the DNA synthesis of prenatal and postnatal aging mouse retina after labeled thymidine injection. *Cellular and Molecular Biology*, 38: 661-668.
151. Kong Y, Usuda N & Nagata T (1992). Radioautographic study on DNA synthesis of the retina and retinal pigment epithelium of developing mouse embryo. *Cellular and Molecular Biology*, 38: 263-272.
152. Kong Y (1993). Electron microscopic radioautographic study on DNA synthesis in perinatal mouse retina. *Cellular and Molecular Biology*, 39: 55-64.
153. Gao F, Toriyama K, Ma H & Nagata T (1993). Light microscopic radioautographic study on DNA synthesis in aging mice cornea. *Cellular and Molecular Biology*, 39: 435-441.
154. Kong Y, Usuda N, Morita T, Hanai T & Nagata T (1992). Study on RNA synthesis in the retina and retinal pigment epithelium of mice by light microscopic radioautography. *Cellular and Molecular Biology*, 38: 669-678.
155. Toriyama K (1995). Study on the aging changes of DNA and protein synthesis of bipolar and photo-receptor cells of mouse retina by light and electron microscopic radioautography. *Cellular and Molecular Biology*, 41: 593-601.
156. Nagata T, Cui H & Gao F (1995). Radioautographic study on glycoprotein synthesis in the ocular tissues. *Journal of Kaken Eye Research*, 14: 11-18.
157. Yamada A & Nagata T (1992). Light and electron microscopic radioautography of DNA synthesis in the endometria of pregnant-ovariectomized mice during activation of implantation window. *Cellular and Molecular Biology*, 38: 763-774.
158. Yamada A & Nagata T (1993). Light and electron microscopic radioautographic studies of RNA synthesis of periimplanting pregnant mouse uterus during activation of receptivity for blastocyst implantation. *Cellular and Molecular Biology*, 39: 221-233.
159. Yamada A (1993). Timely and topologically defined protein synthesis in the peri-implanting mouse endometrium revealed by light and electron microscopic radioautography. *Cellular and Molecular Biology*, 39: 1-12.
160. Uwa H & Nagata T (1976). Cell population kinetics of the scleroblasts during ethisterone-induced anal-fin process formation in adult females of the medaka, *Oryzias latipes*. *Development Growth and Differentiation*, 18: 279-288.
161. Oguchi K & Nagata T (1980). A radioautographic study of activated satellite cells in dystrophic chicken muscle. In: The Ministry of Welfare of Japan (Editor), *Current Research in Muscular Dystrophy Japan. Annual Report on Neurological Diseases 1980*. Tokyo, Japan, 16-17.
162. Oguchi K & Nagata T (1981). Electron microscopic radioautographic observation on activated satellite cells in dystrophy chickens. In: The Ministry of Welfare of Japan (Editor), *Current Research in Muscular Dystrophy Japan. Annual Report on Neurological Diseases 1981*. Tokyo, Japan, 30-33.
163. Sakai Y, Ikado S & Nagata T (1977). Electron microscopic radioautography of satellite cells in regenerating muscles. *Journal of Clinical Electron Microscopy*, 10: 508-509.
164. Yoshizawa S, Nagata A, Honma T, Oda M, Murata F & Nagata T (1974). Study of ethionine pancreatitis by means of electron microscopic radioautography. *Journal of Clinical Electron Microscopy*, 7: 349-350.
165. Yoshizawa S, Nagata A, Honma T, Oda M, Murata F & Nagata T (1977). Radioautographic study of protein synthesis in pancreatic exocrine cells of alcoholic

rats. *Journal of Clinical Electron Microscopy*, 10: 372-373.
166. Fujii Y, Ohno S, Yamabayashi S, Usuda N, Saito H, Furuta S & Nagata T (1980). Electron microscopic radioautography of DNA synthesis in primary cultured cells from an IgG myeloma patient. *Journal of Clinical Electron Microscopy*, 13: 582-583.
167. Murata F, Momose Y, Yoshida K, Ohno S & Nagata T (1977). Nucleic acid and mucosubstance metabolism of mastocytoma cells by means of electron microscopic radioautography. *Acta Pharmacologica et Toxicologica*, 41: 58-59.
168. Nagata T, Iwadare I & Murata F (1977). Electron microscopic radioautography of nucleic acid synthesis in cultured cells treated with several carcinogens. *Acta Pharmacologica et Toxicologica*, 41: 64-65.
169. Ullberg S (1954). Studies on the distribution and fate of 35S-labelled benzylpenicillin in the body. *Acta Radiologica*, 118 (Suppl): 1-110.
170. Nagata T, Yoshida K, Ohno S & Murata F (1978). Ultrastructural localization of soluble and insoluble ^{3}H-methyl prednisolone as revealed by electron microscopic dry-mounting radioautography. *Proceedings of the 9th International Congress on Electron Microscopy*, 2: 40-41.
171. Tsukahara S, Yoshida K & Nagata T (1980). A radioautographic study on the incorporation of ^{14}C-bupranolol (beta-blocking agent) into the rabbit eye. *Histochemistry*, 68: 237-244.
172. Yamabayashi S, Gunarso W, Tsukahara S & Nagata T (1981). Incorporation of ^{3}H-befunolol (beta-blocking agent) into melanin granules of ocular tissues in the pigmented rabbits. I. Light microscopic radioautography. *Histochemistry*, 73: 371-375.
173. Nagata T & Yamabayashi S (1983). Intracellular localization of ^{3}H-befunolol by means of electron microscopic radioautography of cryo-fixed ultrathin sections. *Journal of Clinical Electron Microscopy*, 16: 737-738.
174. Momose Y, Naito J & Nagata T (1989). Radioautographic study on the localization of an anti-allergic agent, tranilast, in the rat liver. *Cellular and Molecular Biology*, 35: 347-355.
175. Momose Y & Nagata T (1993). Radioautographic study on the intracellular localization of a hypolipidemic agent, bezafibrate, a peroxisome proliferator, in cultured rat hepatocytes. *Cellular and Molecular Biology*, 39: 773-781.
176. Momose Y, Naito J, Suzawa H, Kanzawa M & Nagata T (1995). Radioautographic study on the intracellular localization of bezafibrate in cultured rat hepatocytes. *Acta Histochemica et Cytochemica*, 28: 61-66.
177. Nishigaki T, Momose Y & Nagata T (1990). Localization of the anti-allergic agent tranilast in the urinary bladder of rat as demonstrated by light microscopic radioautography. *Drug Research*, 40: 272-275.
178. Hidaka H, Sasaki Y, Tanaka T, Endo T, Ohon S, Fujii Y & Nagata T (1981). N-(6-aminohexyl)-5-chloro-1-naphthalenesulfonamide, a calmodulin antagonist, inhibits cell proliferation. *Proceedings of the National Academy of Sciences, USA*, 78: 4354-4357.
179. Ohno S, Fujii Y, Usuda N, Endo T, Hidaka H & Nagata T (1983). Demonstration of intracellular localization of calmodulin antagonist by wet-mounting radioautography. *Journal of Electron Microscopy*, 32: 1-12.
180. Suzuki K, Imada T, Gao F, Ma H & Nagata T (1994). Radioautographic study of benidipine hydrochloride: localization in the mesenteric artery of spontaneously hypertensive rat. *Drug Research*, 44: 129-133.
181. Usuda N, Nagata T, Naka M & Hidaka H (1985). The localization of a new antithrombotic agent, cilostazol, in CHO-K1 cells as demonstrated by radioautography. *Drug Research*, 35: 1141-1143.